IIR FILTERING APPROACH FOR OPTICAL PULSE PROPAGATION SIMULATION

Time Domain Infinite Impulse Response Filtering Approach for Simulation of Pulse Propagation in Optical Fiber with PMD

By

HONGJING ZHAO
B. ENG. M. ENG

A Thesis
Submitted to the School of Graduate Studies
in Partial Fulfillment of the Requirements
for the Degree
Master of Applied Science

McMaster University

MASTER OF APPLIED SCIENCE (2005) MCMASTER UNIVERSITY
(Electrical and Computer Engineering) Hamilton, Ontario

TITLE: Time Domain Infinite Impulse Response Filtering Approach for Simulation of Pulse Propagation in Optical Fiber with PMD

AUTHOR: Hongjing Zhao, B. Eng. M. Eng. (Beijing Jiaotong University)

SUPERVISOR: Professor Xun Li

NUMBER OF PAGES: vi, 66

Acknowledgements

I would like to express my profound gratitude and high regards to my advisor, Professor Xun Li. His encouragement, suggestions and support during the course of this research have played a vital role. I have learned from him not only the knowledge but also the invaluable methodologies to solve problems. I could not complete my thesis and research without his guidance. I would then like to thank Professor Wei-Ping Huang and Professor Shiva Kumar from whom I learned a lot in photonic device and communication system fields during my study period. I would also like to thank the other members in our group. Their friendship and kindness accompany my study and research.

Finally, it is impossible to finish this thesis without the continuous love and support from my family. I appreciate my husband for his encouragement and assistance which make me go through years of graduate study. I would like to give my special thanks to my parents, Huicun Zhao and Rongzhen Shen, my sisters, Hongyan Zhao and Hongrui Zhao. To all of them, I dedicate this thesis.

Abstract

In this thesis, we have developed a full time domain approach for the simulation of pulse propagation in the optical fiber. Same as split-step method in frequency domain, this approach also treats the linear and nonlinear process alternately. To avoid the back and forth transformation between time and frequency domains, a digital Infinite Impulse Response (IIR) filter is used to treat the linear propagation directly in time domain. The signal samples pass through a pre-extracted IIR digital filter where the convolution is simply replaced by a series of operations that consist of shift and multiplication only.

Compared with frequency domain method, this approach is fully realized in a "data-flow" fashion. Compared with time domain finite impulse response (FIR) method, this approach can save more memory and computation time.

This approach is verified by comparing with the conventional frequency domain split-step Fourier method, and it is applied to the simulation of the pulse propagation, including polarization mode dispersion (PMD) effect in the optical fiber.

Table of Contents

Chapter 1

Introduction

1.1 Optical Fiber Communication System

Optical fiber communication systems have attracted more and more attention in the recent years because optical fibers have so many outstanding advantages. The most significant merit of an optical fiber is its enormous bandwidth. An optical fiber communication system uses a very high carrier frequency, around 200THz [1], which provides a far greater potential bandwidth than a cable system. Coaxial cables have a bandwidth up to approximately 500MHz [2]. In optical systems, this carrier frequency is usually expressed as a wavelength, $1.55\mu m$. This enormous bandwidth makes it possible to transmit signals at a very high speed.

Fiber loss and dispersion are two primary constraints in optical fiber communication systems. The fiber loss is reduced to $0.2 dB/km$ in the early 1970's, and the invention of the Erbium-Doped Fiber Amplifier (EDFA) in the late 1980's brought a whole new era of lightwave communications. After that, dispersion in fibers became the major constraint in optical communication system instead of the fiber loss. And as the transmission rate continually increases, the random birefringence in the optical fiber cannot be ignored because it leads to a phenomenon called Polarization Mode Dispersion (PMD). When the single channel bit rate grows beyond $10 Gbit/s$, PMD becomes a major concern and limitation in optical communication systems. Because of the advanced manufacturing

process which makes PMD very low, we can have system working at bit rate of $40Gbps$ per channel. Anyway, when the speed continues to increase beyond $40Gbps$, PMD will be significant and cannot be ignored.

Most optical fiber communication systems nowadays use intensity modulation-direct detection (IM/DD). A typical multi-span fiber system is shown in Figure 1.1.

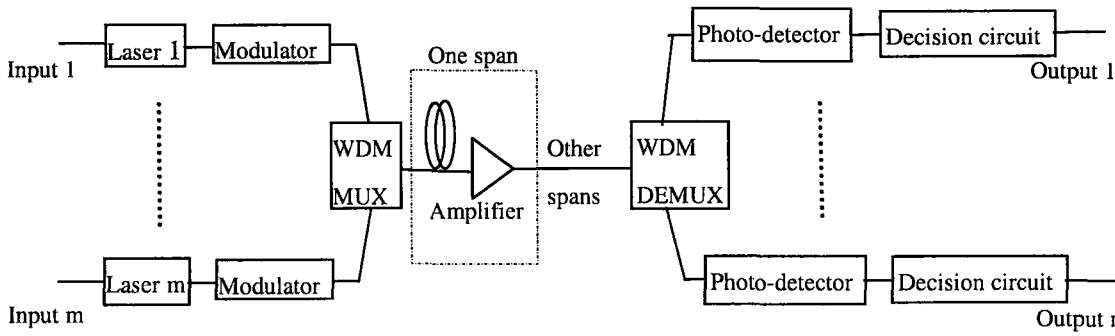

Figure 1.1 A schematic diagram of an optical fiber communication system

At the transmitter side, single or multiple lasers are used as the transmitters. Directly modulating laser diodes or external modulators can be used. The input signal can be of any waveform such as Gaussian, rectangular or raise-cosine. An EDFA or semiconductor optical amplifier (SOA) is also used right after the transmitter in some systems to increase the signal power for further propagation. If wavelength-division multiplexing (WDM) system is used, a multiplexer (MUX) is needed before transmitting the signals through fiber spans.

As the signal propagates through the optical fiber, it will be distorted and needs another amplifier to extend the propagation length without using repeater. The signal will

then propagate along the fiber again and reach the receiver end. At the receiver side, the photo-detector, along with the decision circuit, converts the received optical signal to the electrical output. If WDM is used, before the photo-detector the signal will pass through a WDM demultiplexer (DEMUX), which is used to effectively separate the signal.

Although manufacturing technology is very mature and standardized today, it is still very expensive to build the real system. Computer modeling and simulation are having, and will increasingly have, a pivotal role in supporting the design of long-haul amplified terrestrial and submarine systems, as well as of medium- and short-length ultrahigh-capacity ($Tbit/s$) systems. In all these instances, the trial-and-error experimentation of several different design solutions has become unrealistic due to the overwhelming cost of the testbeds. It is also necessary that the indispensable testbeds be immediately functional, and only small adjustments are needed to reach the final configuration in the actual system. The only way is to precede the testbed implementation phase with a thorough modeling and simulation method that allows the fine adjustment of the system parameters in advance [4]. System performance simulations become more important in the development of the new systems and in the optimization of the existing ones. In studying pulse propagation in optical fiber, especially incorporating the polarization mode dispersion effect, a computational effective simulation is very necessary.

1.2 Thesis Motivation

Pulse propagation in optical fiber is governed by the well-known Nonlinear

Schrodinger Equation (NSE). This equation is a nonlinear partial differential equation (PDE) that generally does not have analytical solutions except for a few special cases in which the inverse scattering method can be used. Therefore, a numerical method is very necessary. A large number of numerical methods have been developed [2]-[10]. Among them, frequency domain split-step method [3][10] is the most popular. Recently, a time domain split-step digital FIR filtering method has been developed [11]. After that, this time domain split-step digital FIR filtering method was further applied to the situation incorporating the polarization mode dispersion effect [12]. If the mappings from frequency domain transfer functions to time domain filters need be done at every step, the extra burden due to the filter extraction will offset all the computation effort saved by using time domain approach. To solve this problem, this approach was developed. The key idea of this approach is to extract the FIR filter coefficients for all the possible transfer functions at the very beginning just once to establish a one-to-one mapping from the frequency domain transfer functions to the time domain filters, then to call the relevant time domain filter when the frequency domain transfer function is randomly selected in the propagation.

In this thesis, a time domain split-step digital IIR filtering approach is proposed for the evaluation of the optical pulse propagation along the fiber. Similar to the time domain split-step digital FIR filtering approach, IIR approach also has the following advantages: It can provide a data flow fashion to simulate the pulse propagation in optical fiber; it makes the noise treatment much easier; it makes the distributed and parallel computing possible; it meets causality requirement automatically, as the output signal sample will

depend on the past input and output signal sample only. But in computation complexity, this IIR filtering approach is really superior to FIR filtering approach.

For a given sampling interval and a given resolution on fiber frequency domain response, a feature number N can be extracted as one over the product of the time domain sampling interval and the frequency domain resolution. The computation complexity is $O(N \log N)$ for frequency domain FFT algorithm and $O(N^2)$ for time domain convolution algorithm.

In digital filtering algorithms, if a filter with length N contains redundant information, however, this filter always can be replaced by a different filter with a reduced length $M(< N)$ without noticeable accuracy sacrifice. For instance, the IIR filter can be employed to replace the FIR filter with a greatly reduced filter length. The FIR filter built on Chebyshev polynomials can also reduce the length of that built on the normal Tyler series [13]. Therefore, the time domain digital filter algorithm will be computationally less complex than the frequency domain FFT algorithm as long as the filter length is $M < \sqrt{N \log N}$ [14].

The computation complexity is $O((2(P+1))^2)$ for time domain IIR filtering approach, where P is the order of IIR filter. Under the same condition, compared with FIR filter, IIR filter always can fit frequency domain transfer function with fewer terms. The IIR filter proposed in this thesis only includes four items ($P=1$), which is yet realized at the cost of bandwidth. Therefore, we have to reduce step size, that is, increase the number of the step n for the same fiber span to ensure enough bandwidth. The

computation complexity of FIR approach is $O(M^2)$, increasing quadratically with the length of FIR filter, while the computation complexity of IIR approach is $O(n(2(P+1))^2) = O(4n)$, increasing linearly with the number of the step. Thus, split-step IIR filtering approach will save more memory and computation time than split-step FIR filtering approach.

We will apply this work to the simulation of pulse propagation over optical fibers with the PMD effect where coupled nonlinear Schrodinger equations (CNSE) must be solved.

1.3 Outline of Thesis

This thesis is organized in such a way: Firstly, polarization mode dispersion and governing equations for pulse propagation in optical fiber are described in chapter 2. In chapter 3, frequency domain split-step FFT method and time domain split-step FIR method for solving the nonlinear Schrodinger equation (NSE) and coupled nonlinear Schrodinger equations (CNSE) are reviewed. Time domain split-step IIR method for solving the NSE is described, and some implementation examples are given in chapter 4. The proposed time-domain split-step IIR filtering approach for solving CNSE is described in chapter 5. The implementations of split-step IIR filtering approach for CNSE are validated through comparisons in chapter 6. In Chapter 7, final conclusions are summarized and future work is proposed.

Chapter 2

Polarization Mode Dispersion and Governing Equations

2.1 PMD in Optical Fiber

Single-mode fiber supports one fundamental mode, which consists of two orthogonal polarization modes, the fast mode and the slow mode, due to birefringence which is caused by internal or external stresses or by non-perfect circularity of the fiber core. Mechanical stress exerted on the fiber during cabling, installing, and splicing, as well as the imperfections arise in the manufacturing process, are the reason for the variations in the cylindrical geometry. The asymmetry of the fiber core introduces small refractive index difference for the two polarization states. Each polarization mode has its own propagation constant. Usually the state of polarization of an arbitrary optical field can be represented by the vector sum of the field components aligned with the two polarization modes.

The difference in propagation constants is called birefringence strength,

$$\Delta\beta = \left|\beta_s - \beta_f\right| = \left|\frac{\omega n_s}{c} - \frac{\omega n_f}{c}\right| = \frac{\omega}{c}\Delta n_{eff} \quad (2.1)$$

where $\Delta\beta$ is birefringence strength;

β_s is the propagation constant of the slow mode;

β_f is the propagation constant of the fast mode;

Δn_{eff} is the differential index of fraction;

n_s is the effective index of refraction of the slow mode and defined as $n_s = \frac{c\beta_s}{\omega}$;

n_f is the effective index of refraction of the fast mode and defined as $n_f = \frac{c\beta_f}{\omega}$;

c is the speed of light, $3\times10^8\ m/s$.

The degree of modal birefringence B is defined by

$$B = \frac{|\beta_s - \beta_f|}{k_0} = |n_s - n_f| \quad (2.2)$$

For a given value of B, the power between the two modes exchanges periodically as they propagate inside the fiber with the period L_{beat} defined by

$$L_{beat} = \frac{2\pi}{|\beta_s - \beta_f|} = \frac{\lambda}{B} \quad (2.3)$$

L_{beat} is generally referred to as the beat length. The axis along which the effective mode index is smaller is called fast axis as the group velocity is larger for light propagating in that direction. For the same reason, the axis with a larger mode index is called slow axis.

v_g is defined as group velocity at which a particularly marked spot on a low-frequency envelope will be seen to move at

$$v_g = \left(\frac{d\omega}{d\beta}\right) \quad (2.4)$$

The different group velocities of the modes cause the optical pulse broadening. Therefore, they limit the bandwidth of the optical fiber communication system. The difference in the group delays between the fast and slow modes is

$$\Delta\tau = \left|\frac{d(\Delta\beta)}{d\omega}\right| = \left|\frac{\Delta n_{eff}}{c} - \frac{\omega}{c}\frac{d\Delta neff}{d\omega}\right| \quad (2.5)$$

where $\Delta\tau$ is also called the differential group delay (DGD).

Because birefringence exists, if input pulse excites both polarization components, it becomes broader at the fiber output side since the two components disperse along the fiber due to the DGD. This phenomenon is called Polarization Mode Dispersion (PMD). And the delay between the two components is called the DGD. DGD is the unit which is

used to describe PMD. PMD can be categorized as first order PMD and second order PMD. The second order PMD is the result of the signal's wavelength dependence and pulse broadening.

PMD can be ignored at low bit rate but becomes important as the bit rate continues to increase. PMD is a significant source of impairment for ultra-long-haul transmission at high bit rates. It becomes of considerable concern as the bit rate of each channel in system goes beyond $10Gbps$. The performance of long-haul $40Gbps$ systems would be limited by PMD, and the situation would become worse as the bit rate continues to increase [15][16].

2.2 Governing Equations

Pulse propagation in optical fiber is governed by the well-known Nonlinear Schrodinger Equation (NSE). This equation is used to describe the slowly-varying envelope of the optical field.

On the other hand, when fiber birefringence is not negligible, a single NSE is not sufficient for describing the behavior of pulse propagation in such fibers [17]. The birefringence in optical fiber leads to PMD which changes randomly over time and wavelength. Its effect is also polarization dependent, which makes the description of the pulse propagation rather complicated as polarization related statistics must be involved. As a result, the simulation of pulse propagation including the PMD effect must be computationally much more expensive as the fiber property virtually changes from

section to section. A related problem with the conventional frequency domain split-step Fourier method is the drastic increase of the back and forth Fast Fourier Transform (FFT) with huge memory size and tremendous computation time involved.

2.2.1 Nonlinear Schrodinger Equation

From Maxwell's equations, we can obtain the wave equation that describes lightwave propagation in optical fibers. Starting from the wave equation, we can derive a basic equation that governs the propagation of slowly-varying envelope of the lightwave in nonlinear dispersive fibers, namely, the nonlinear Schrodinger equation (NSE) [18],

$$\frac{\partial \overline{A}}{\partial z} + \frac{\alpha}{2}\overline{A} + \beta_1 \frac{\partial \overline{A}}{\partial t} + \frac{i}{2}\beta_2 \frac{\partial^2 \overline{A}}{\partial t^2} - \frac{1}{6}\beta_3 \frac{\partial^3 \overline{A}}{\partial t^3} = i\gamma \left|\overline{A}\right|^2 \overline{A} \qquad (2.6)$$

where $\overline{A}$ denotes the envelope of the lightwave;

α denotes the fiber loss;

β_1 denotes the wave propagation constant;

β_2 denotes the fiber second-order dispersion;

β_3 denotes the fiber third-order dispersion;

γ denotes the fiber nonlinear parameter;

i represents the imaginary unit.

When other effects, such as PMD effect, are considered, the basic NSE equation will be made some changes correspondingly.

In equation (2.6), the dispersions higher than the third order are generally neglected. This simplification is consistent with the quasi-monochromatic assumption in the derivation from Maxwell's equations to NSE equation. Some transformations are further made to make this equation (2.6) more simple and clear.

It is useful to use a reference moving with the pulse at the group velocity v_g (retarded time) to eliminate β_1 from the real time,

$$T = t - \beta_1 z \quad (2.7)$$

Then, the envelope is scaled to explicitly cancel out the homogenous loss to further simplify the governing equation,

$$\overline{A} = Ae^{-\frac{\alpha}{2}z} \quad (2.8)$$

Finally the nonlinear Schrodinger equation (NSE) becomes:

$$\frac{\partial A}{\partial z} + i\frac{\beta_2}{2}\frac{\partial^2 A}{\partial T^2} - \frac{\beta_3}{6}\frac{\partial^3 A}{\partial T^3} - i\gamma e^{-\alpha z}|A|^2 A = 0 \qquad (2.9)$$

This equation is valid for pulse whose width is $\geq 0.1ps$ ($\Delta\omega \leq 10^{13} s^{-1}$).

2.2.2 Coupled Nonlinear Schrodinger Equation

When fiber birefringence becomes a major concern, the coupled nonlinear Schrodinger equations (CNSE) are the governing equations that describe pulse propagation in optical fiber [19]. In this thesis we select the form in which birefringence orientation varies randomly and the birefringence strength is fixed in each step. Later this will be described in detail.

$$\frac{\partial \bar{U}_1}{\partial z}+\frac{\alpha}{2}\bar{U}_1-ib\left(\bar{U}_1\cos\theta+\bar{U}_2\sin\theta\right)+b'\left(\frac{\partial \bar{U}_1}{\partial T}\cos\theta+\frac{\partial \bar{U}_2}{\partial T}\sin\theta\right)+\frac{i}{2}\beta_2\frac{\partial^2 \bar{U}_1}{\partial T^2}-i\gamma\left|\bar{U}_1\right|^2\bar{U}_1+\gamma\frac{i}{3}\left(\left|\bar{U}_2\right|^2\bar{U}_1-\bar{U}_1^*\bar{U}_2^2\right)=0$$

$$\frac{\partial \bar{U}_2}{\partial z}+\frac{\alpha}{2}\bar{U}_2-ib\left(\bar{U}_1\sin\theta-\bar{U}_2\cos\theta\right)+b'\left(\frac{\partial \bar{U}_1}{\partial T}\sin\theta-\frac{\partial \bar{U}_2}{\partial T}\cos\theta\right)+\frac{i}{2}\beta_2\frac{\partial^2 \bar{U}_2}{\partial T^2}-i\gamma\left|\bar{U}_2\right|^2\bar{U}_2+\gamma\frac{i}{3}\left(\left|\bar{U}_1\right|^2\bar{U}_2-\bar{U}_2^*\bar{U}_1^2\right)=0$$

(2.10)

Where $\bar{U}_1, \bar{U}_2$ denotes the complex envelope of two polarization components of the optical field;

T is the retarded time $T = t - \beta_1 z$. This transformation is important in simulation because it allows one to view the signal propagate in a time window of limited duration;

α denotes the fiber loss;

b is the birefringence parameter which is defined as $b = \frac{\pi}{L_{beat}}$, and measured in m^{-1};

L_{beat} is the beat length of the fiber given as $L_{beat} = \frac{\lambda}{\Delta n}$, and measured in m, where λ is the wavelength and Δn is typically 10^{-7};

b' is given by $b' = \frac{D_{PMD}}{2(2L_{corr})^{\frac{1}{2}}}$, and measured in $ps/(km \cdot m)^{\frac{1}{2}}$;

D_{PMD} denotes the polarization mode dispersion coefficient, and is measured in $ps/(km)^{\frac{1}{2}}$;

L_{corr} is the fiber correlation length, and measured in m;

β_2 is the second order dispersion;

γ is the fiber nonlinear parameter, given as $\gamma = \frac{\omega_0 n_2}{cA_{eff}}$ where ω_0, n_2, A_{eff} are the central frequency, nonlinear coefficient and effective mode area, respectively; γ is measured in W^{-1}/km;

i represents the imaginary unit.

Without losing generality, the dispersions higher than the second order are still neglected here. But one can easily modify equation (2.10) to incorporate other physical effects if necessary.

The similar transformations are made to the equation (2.10)

$$\begin{aligned} \overline{U_1} &= U_1 \exp\left(-\frac{\alpha}{2}z\right) \\ \overline{U_2} &= U_2 \exp\left(-\frac{\alpha}{2}z\right) \end{aligned} \qquad (2.11)$$

to eliminate the loss term. The following simplified equations can be gotten

$$\begin{aligned} &\frac{\partial U_1}{\partial z} - ib(U_1\cos\theta + U_2\sin\theta) + b'\left(\frac{\partial U_1}{\partial T}\cos\theta + \frac{\partial U_2}{\partial T}\sin\theta\right) + \frac{i}{2}\beta_2\frac{\partial^2 U_1}{\partial T^2} - i\gamma\exp(-\alpha z)\left(|U_1|^2 U_1 + \frac{i}{3}\exp(-\alpha z)\left(|U_2|^2 U_1 - U_1^* U_2^2\right)\right) = 0 \\ &\frac{\partial U_2}{\partial z} - ib(U_1\sin\theta - U_2\cos\theta) + b'\left(\frac{\partial U_1}{\partial T}\sin\theta - \frac{\partial U_2}{\partial T}\cos\theta\right) + \frac{i}{2}\beta_2\frac{\partial^2 U_2}{\partial T^2} - i\gamma\exp(-\alpha z)\left(|U_2|^2 U_2 + \frac{i}{3}\exp(-\alpha z)\left(|U_1|^2 U_2 - U_2^* U_1^2\right)\right) = 0 \end{aligned} \qquad (2.12)$$

On the left hand side, the second term and third term represent the contributions from the fiber birefringence to the signal; if these terms are not zero, the signals undergo polarization mode dispersion. The parameter b and θ are the birefringence parameter and birefringence orientation angle, respectively. It is important to note that both parameters are random. Virtually, it is reasonable to view the fiber as a linked segments whose length are small enough that their birefringence can be considered constant inside each segment [17]. Within each segment, the birefringence is deterministic, that is, changes only occur from section to section. Thus, random coupling between two polarization components occurs only between different fiber sections because of the random rotation of the principal axis. There are two specific physical models to capture this randomness. In the first model, the birefringence orientation varies randomly from

section to section while the birefringence strength is fixed. In the second model, both the birefringence strength and orientation change randomly from section to section. The two components are assumed to be Gaussian random processes, statistically independent of each other [20]. It has been shown that both models will lead to identical result [21]. In this thesis, the first model will be selected for our simulation because it makes the treatment easier.

The forth term takes into account the second order dispersion. The fifth term is referred to as nonlinearity effect with the loss term included.

The very last term is the polarization mode coupling effect between the two components. The power exchange between the two polarizations mode are linked through this term. Mathematically, the coupling effect between them is linked through a transfer matrix. This matrix includes the rapid motion over the Poincare sphere which completely characterize the parameters underlying polarization mode dispersion within a given optical frequency range in the fiber.

Chapter 3

Split-step FFT and FIR-DSP Methods

3.1 Frequency Domain Split-step FFT Method

The basic idea of split-step FFT method is to divide the fiber span into many steps. Within each step, the linear and nonlinear effects are pretended to act alternately. To understand how this method works, it is useful to rewrite nonlinear Schrodinger equation (2.6) as

$$\frac{\partial A}{\partial t} = (D+N)A \quad (3.1)$$

where D is the linear operator that accounts for dispersion and N is the nonlinear operator that governs the nonlinear effect. In particular,

$$\begin{aligned} D &= -i\frac{\beta_2}{2}\frac{\partial^2}{\partial T^2} + \frac{\beta_3}{6}\frac{\partial^3}{\partial T^3} \\ N &= i\gamma e^{-\alpha z}|A|^2 \end{aligned} \quad (3.2)$$

In every small propagation step, these two operations are assumed to take effects alternately [18], then the dispersion and nonlinear effects can be treated independently. That is, the calculation is made up of two separated steps. The solution to equation (2.6) is given by [6],

$$\tilde{A}(z+\Delta z,\omega)=H_D F\left[A(z,T)\right] \quad (3.3)$$

$$A(z+\Delta z,T)=\exp\left(i\Delta z\gamma e^{-\alpha z}\left|F^{-1}\left[\tilde{A}(z+\Delta z,\omega)\right]\right|^2\right)F^{-1}\left[\tilde{A}(z+\Delta z,\omega)\right] \quad (3.4)$$

where $F[\ ]$ and $F^{-1}[\ ]$ denote the Fourier and inverse Fourier transform respectively, and the frequency domain transfer function in equation (3.3) is given by

$$H_D(\omega)=e^{i(\frac{1}{2}\beta_2\Delta z\omega^2-\frac{1}{6}\beta_3\Delta z\omega^3)} \quad (3.5)$$

Equation (3.3) to (3.5) is the core of the split-step Fourier algorithm.

It is clear that the solution from split-step method converges to the exact solution of (2.6) as the step size decreases to 0. It is also known that the error introduced in each step is in the order of Δz^2. Throughout this thesis, the results from frequency domain Split-step method are assumed to be the exact solutions to the NSE equation and are used as a basis for comparison with the results from our simulation and analysis.

3.2 Time Domain Split-step FIR-DSP Method

A general FIR digital filter approach is used to treat the linear propagation directly in time domain, which can keep a good balance between the computation efficiency and accuracy [11].

Firstly, a FIR filter is extracted. This makes all processes be treated in time domain without much sacrifice on the accuracy. A polynomial function is constructed

$$\hat{H}_F(\omega) = \sum_{k=0}^{M} h_k e^{i\omega\Delta k} \qquad (3.6)$$

where Δ denotes the time domain sampling interval and $h_0, h_1, h_2, \ldots h_M$ are the coefficients of FIR filter, which need to be calculated by searching for the linear least square fit to the frequency domain transfer function $H_D(\omega)$. A standard merit function can be defined as

$$\chi^2 = \sum_{l=1}^{L}\left[H_D(\omega_l) - \hat{H}_F(\omega_l)\right]^2 = \sum_{l=1}^{L}\left[H_D(\omega_l) - \sum_{k=0}^{M} h_k e^{i\omega\Delta k}\right]^2 \qquad (3.7)$$

Where $\omega_l, l = 1,2,3\ldots,L$ are a frequency domain sampling set, which uniformly covers the entire interested frequency range Ω determined by the spectrum of the input signal.

Let $\partial\chi^2 / \partial h_k = 0$, $k = 0,1,2\ldots M$, which yields

$$\begin{bmatrix} \sum_{l=1}^{L} 1 & \sum_{l=1}^{L} e^{iw_l\Delta} & \cdots & \sum_{l=1}^{L} e^{iw_l\Delta} \\ \sum_{l=1}^{L} e^{iw_l\Delta} & \ddots & \cdots & \vdots \\ \vdots & \vdots & \ddots & \vdots \\ \sum_{l=1}^{L} e^{iw_l\Delta M} & \sum_{l=1}^{L} e^{iw_l\Delta(M+1)} & \cdots & \sum_{l=1}^{L} e^{iw_l\Delta 2M} \end{bmatrix} \begin{bmatrix} h_0 \\ h_1 \\ \vdots \\ h_M \end{bmatrix} = \begin{bmatrix} \sum_{l=1}^{L} H_D(w_l) \\ \sum_{l=1}^{L} e^{iw_l\Delta} H_D(w_l) \\ \vdots \\ \sum_{l=1}^{L} e^{iw_l\Delta M} H_D(w_l) \end{bmatrix} \quad (3.8)$$

By solving this linear equation (3.8), FIR coefficients $h_0, h_1, \cdots, h_M$ can be calculated. M should be selected as the smallest integer that makes the error χ^2 smaller than a pre-given value. This can be easily done by looping M in an ascent order.

Replacing (3.5) by (3.6) in (3.3) gives

$$\tilde{A}(z+\Delta z,\omega) = \sum_{k=0}^{M} h_k e^{i\omega\Delta k} F[A(z,T)] \quad (3.9)$$

Convert equation (3.9) back to time domain

$$F^{-1}[\tilde{A}(z+\Delta z,\omega)] = \sum_{k=0}^{M} h_k A(z,T-k\Delta) \quad (3.10)$$

Finally, equation (3.10) and (3.4) form the time domain split-step FIR filtering algorithm, where the linear propagation is evaluated through a digital FIR filter with length $M+1$.

3.3 Split-step FFT method for CNSE

Similar to the way to solve the NSE, only this time the split-step Fourier method is applied to solve a pair of nonlinear Schrodinger equations.

Still using the split-step Fourier method to separate the linear and the nonlinear operators, the coupled nonlinear Schrodinger equation (2.12) can be written as

$$\begin{aligned} \frac{\partial U_1}{\partial z} &= (N_1 + D)U_1 \\ \frac{\partial U_2}{\partial z} &= (N_2 + D)U_2 \end{aligned} \qquad (3.11)$$

where D is the linear operator, N_1 and N_2 are the nonlinear operators for two different polarization envelopes :

$$D = -i\frac{1}{2}\beta_2\frac{\partial^2}{\partial T^2} \qquad (3.12)$$

$$\begin{aligned} N_1 &= i\gamma\exp(-\alpha z)\left[|U_1|^2 - \frac{1}{3}\left(|U_2|^2 - \frac{U_1^*}{U_1}U_2^2\right)\right] \\ N_2 &= i\gamma\exp(-\alpha z)\left[|U_2|^2 - \frac{1}{3}\left(|U_1|^2 - \frac{U_2^*}{U_2}U_1^2\right)\right] \end{aligned} \qquad (3.13)$$

The operators D, N_1 and N_2, still take effects alternately over a small propagation

distance Δz, and the dispersion and nonlinear effects can be considered independently. Thus, the computation still includes two steps: linear step and nonlinear step.

3.3.1 Linear step

In this step, only linear part takes effect while nonlinear part is not considered. CNSE can be expressed as,

$$\begin{aligned}\frac{\partial U_1}{\partial z} &= ib\left(U_1\cos\theta + U_2\sin\theta\right) - b'\left(\frac{\partial U_1}{\partial T}\cos\theta + \frac{\partial U_2}{\partial T}\sin\theta\right) + DU_1 \\ \frac{\partial U_2}{\partial z} &= ib\left(U_1\sin\theta - U_2\cos\theta\right) - b'\left(\frac{\partial U_1}{\partial T}\sin\theta - \frac{\partial U_2}{\partial T}\cos\theta\right) + DU_2\end{aligned} \tag{3.14}$$

After Fourier transformation, equation (3.14) becomes:

$$\begin{aligned}\frac{\partial U_1}{\partial z} &= ib\left(U_1\cos\theta + U_2\sin\theta\right) - i\omega b'\left(U_1\cos\theta + U_2\sin\theta\right) + \overline{D}U_1 \\ \frac{\partial U_2}{\partial z} &= ib\left(U_1\sin\theta - U_2\cos\theta\right) - i\omega b'\left(U_1\sin\theta - U_2\cos\theta\right) + \overline{D}U_2\end{aligned} \tag{3.15}$$

where $\overline{D} = i\frac{1}{2}\beta_2\omega^2$ (3.16) is the dispersive operator in frequency domain. The solution to equation (3.15) is:

$$\begin{aligned}\overline{U}_1(z+\Delta z,\omega) &= \exp\left(\overline{D}\Delta z\right)\left(m_{11}U_1(z,\omega) + m_{12}U_2(z,\omega)\right) \\ \overline{U}_2(z+\Delta z,\omega) &= \exp\left(\overline{D}\Delta z\right)\left(m_{21}U_1(z,\omega) + m_{22}U_2(z,\omega)\right)\end{aligned} \tag{3.17}$$

where m_{ij} are the elements of 2-by-2 matrix transfer function $m(z,\omega)$ which account for the random fiber birefringence effect.

To calculate (3.17), subdivide each interval Δz into smaller subinterval δz, and in each subinterval

$$m_j = \begin{bmatrix} m_{11}^j & m_{12}^j \\ m_{21}^j & m_{22}^j \end{bmatrix} \qquad (3.18)$$

where

$$\begin{aligned} m_{11}^j &= m_{22}^{j*} = \cos[(b - b'\omega)\delta z] + i\cos(\theta_{jl})\sin[(b - b'\omega)\delta z] \\ m_{12}^j &= m_{21}^j = i\sin(\theta_{jl})\sin[(b - b'\omega)\delta z] \end{aligned} \qquad (3.19)$$

and θ_{jl} are constant in each subinterval but random from subinterval to subinterval.

The total transfer matrix is expressed as:

$$\prod_{j=1}^{N} \exp(\overline{D}\Delta z)\cdot m_j(\omega) \qquad (3.20)$$

where N is the number of subintervals.

3.3.2 Nonlinear step

In this step, only nonlinear part takes effect while linear part is not considered. CNSE can be expressed as:

$$\begin{aligned} \frac{\partial U_1}{\partial z} &= N_1 U_1 \\ \frac{\partial U_2}{\partial z} &= N_2 U_2 \end{aligned} \qquad (3.21)$$

The nonlinear effect is added on as:

$$\begin{aligned} U_1(z+\Delta z,T) &= \exp(\Delta z N_1)\overline{U}_1(z+\Delta z,T) \\ U_2(z+\Delta z,T) &= \exp(\Delta z N_2)\overline{U}_2(z+\Delta z,T) \end{aligned} \qquad (3.22)$$

For each step Δz, these two steps are repeated until a given distance is reached.

3.4 Split-step FIR-DSP method for CNSE

The Split-step DSP method [11] is very successful to solve the NSE effectively. But this implementation only included fundamental physical effects, such as the second and third order dispersion and nonlinearity effects. A further extension incorporating the PMD effect has been developed and proven successfully too [12].

Here we will not give the detail how this time domain split-step FIR-DSP method

works to solve the CNSE. Just as mentioned in chapter 1, the key idea of this approach is to extract the FIR filter coefficients for all the possible transfer functions at the very beginning just once to establish a one-to-one mapping from the frequency domain transfer functions to the time domain filters, then to call the relevant time domain filter when the frequency domain transfer function is randomly selected in the propagation. Assuming that we have K split-steps, N subintervals for each split-step and L possible sample frequency domain transfer functions, the direct approach will have to perform $K \cdot N$ filter extractions since at each subinterval one of the L sample frequency domain transfer function will be used, whereas this time domain FIR filtering approach will need only L time domain filter extractions. In practice, we always have $K \cdot N >> L$. Therefore, the direct approach is obviously wasteful as there must be some frequency domain transfer functions repeatedly extracted. This FIR-DSP approach, however, guarantees minimum number of extractions required to establish the mappings from the frequency domain transfer functions to the time domain filters.

Chapter 4

Split-step IIR-DSP Method for NSE

4.1 The Design of IIR Filter

An IIR filter can be built as a rational function

$$H_I(\omega) = \frac{\sum_{k=0}^{P} a_k e^{jk\Delta\omega}}{1 + \sum_{k=1}^{P} b_k e^{jl\Delta\omega}} \quad (4.1)$$

Given the fact that $H_D(\omega)$ is an all-pass filter, $H_I(\omega)$ should have the same number of zeros and poles symmetrically distributed in the complex $z = e^{i\omega\Delta}$ plane. The numerator and the denominator of the rational function (4.1) therefore have the same order defined as p. The total length of the IIR filter is given as $2(p+1)$ accordingly.

Replacing (3.5) by (4.1) in (3.3) gives

$$\tilde{A}(z + \Delta z, \omega) = \frac{\sum_{k=0}^{P} a_k e^{jk\Delta\omega}}{1 + \sum_{k=1}^{P} b_k e^{jl\Delta\omega}} F[A(z,T)] \quad (4.2)$$

By converting equation (4.2) back to time domain, we have

$$\tilde{A}(z+\Delta z,\omega)=\frac{\sum_{k=0}^{P} a_k e^{jk\Delta\omega}}{1+\sum_{k=1}^{P} b_k e^{jl\Delta\omega}} F[A(z,T)] \quad (4.3)$$

Thus, equation (3.4) and (4.3) form the time domain split-step IIR filtering algorithm, where the linear propagation is evaluated through a digital IIR filter with length $2(p+1)$. In this algorithm, not only the input values in the present and previous p steps $[A(z,T-k\Delta),\ k=0,1,2,...,p]$, but also the output values in the previous p steps $[A(z+\Delta z,T-k\Delta),\ k=1,2,...,p]$ will be used for the evaluation of the present output value $[A(z+\Delta z,T)]$. Comparing with the FIR filter with length M, for the same split-step size, this modified IIR filter algorithm saves both computation time and memory size as its length is reduced to $2(P+1)<M$.

In order to improve the accuracy, a better strategy is to consider the nonlinear effect at the midpoint rather than at the end of each step. Actually the following modified algorithm is implemented

$$\begin{cases} A_{1/2}(z+\Delta z/2,T)=\sum_{k=0}^{P} a_k A(z,T-k\Delta)-\sum_{k=1}^{P} b_k A(z,T-k\Delta) \\ A'_{1/2}(z+\Delta z/2,T)=\exp(\Delta z N)A_{1/2}(z+\Delta z/2,T) \\ A(z+\Delta z,T)=\sum_{k=0}^{P} a_k A'_{1/2}(z+\Delta z/2,T-k\Delta)-\sum_{k=1}^{P} b_k A'_{1/2}(z+\Delta z/2,T-k\Delta) \end{cases} \quad (4.4)$$

The coefficients a_k and b_k are extracted from half-step transfer function given by

$$H_D(\omega) = e^{i(\frac{1}{4}\beta_2 \Delta z \omega^2 - \frac{1}{12}\beta_3 \Delta z \omega^3)} \quad (4.5)$$

For $\frac{\Delta z}{2}$, the transfer function of the second order dispersion is

$$H_D(\omega) = e^{i\frac{1}{4}\beta_2 \Delta z \omega^2} \quad (4.6)$$

It can be modeled as a filter which has a unit amplitude and the following group delay

$$\tau_g = \beta_2 \omega \frac{\Delta z}{2} \quad (4.7)$$

Using IIR filter, it is easy to realize that the transfer function be exactly of unit amplitude throughout the Nyquist frequency domain $\omega \in [-\pi/\Delta, +\pi/\Delta]$, where Δ is time domain sampling interval used in the simulation. It is sufficient that each pole p_j of the transfer function in the Z-transform plane be matched by a zero at $1/p_j$.

For the linear group delay of second-order dispersion, we can use the following IIR filter to approximate it [4]:

$$H_{lin}(z) = p_i p_r \frac{z - j\frac{1}{p_i}}{z - jp_i} \frac{z - \frac{1}{p_r}}{z - p_r} \quad (4.8)$$

where $z = e^{i\omega\Delta}$, Δ is time domain sampling interval. p_i and p_r are real numbers. They must be related as

$$1 = 4\frac{p_i^2\left(1-p_i^2\right)\left(1-p_r\right)^3}{p_r\left(1+p_i^2\right)^3\left(1+p_r\right)} \quad (4.9)$$

which can ensure the amplitude of $H_{lin}(z)$ equal to 1. Thus we just need to consider how to fit its phase from $H_D(\omega)$.

This IIR filter has such form of group delay:

$$\tau_{H_{lin}} = \tau_0 + 2\Delta^2\frac{p_i\left(1-P_i^2\right)}{\left(1+p_i^2\right)^2}\omega + O\left(\omega^3\right) \quad (4.10)$$

Here the first term represents a frequency-independent amount of extra delay that has no importance. The second term is the desired linear group delay. The third term indicates that the error is on the order of ω^3 or higher. The ω^2 term is absent because (4.9) ensures that it is cancelled out.

By carefully selecting Δz and Δ, we can make the linear parts of τ_g and $\tau_{H_{lin}}$ equal, thus this IIR filter will approximate our transfer function.

The linear group delay of this IIR filter is limited to $\frac{1}{2}\Delta^2\omega$. This can be seen by plotting the second term of (4.10) as a function of p_i. If a larger value is needed, we can

either cascade more of these filters or reduce the amount of needed delay by shortening the spatial integration step size Δz [22].

To assess how well the filter performs, the following error function is defined as

$$e(\omega)=\frac{1}{\Delta}\left[\tau_{H_{lin}}-\tau_0-2\Delta^2\frac{p_i\left(1-P_i^2\right)}{\left(1+p_i^2\right)^2}\omega\right] \quad (4.11)$$

Its mean-square value ε over the frequency range $[-(\pi/2\Delta),+(\pi/2\Delta)]$

$$\varepsilon=\frac{\Delta}{\pi}\int_{-(\pi/2\Delta)}^{+(\pi/2\Delta)}\left|e(\omega)\right|^2 d\omega \quad (4.12)$$

which turns out to depend only on p_i, not on T_c. ε is fairly low over the whole range $p_i=\pm 0.31$. At approximately $p_i=\pm 0.282$, the error has two minima. Because we need to ensure τ_g and $\tau_{H_{lin}}$ equal, when β_2 is negative, we select $p_i=-0.282$, and the corresponding $p_r=0.1336$.

We plot the linear group delay implemented by the IIR filter versus idea linear group delay in Figure 4.1, and the phase in Figure 4.2. Here the following parameters are selected: $\beta_2=-22\,ps^2/km$, $\Delta=0.390625ps$, $\Delta z/2=0.0062km$. There is a good agreement between the desired linear group delay and the synthesized one, at least half the Nyquist frequency.

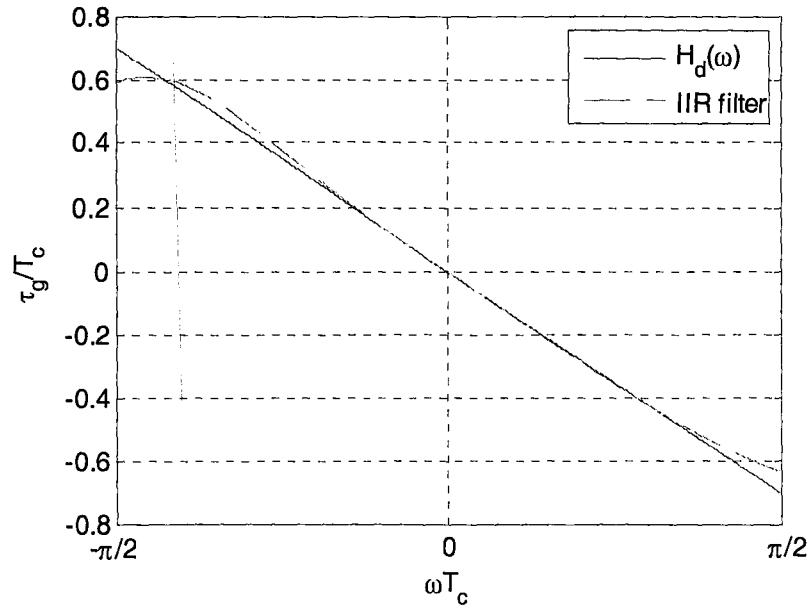

Figure 4.1 linear group delay

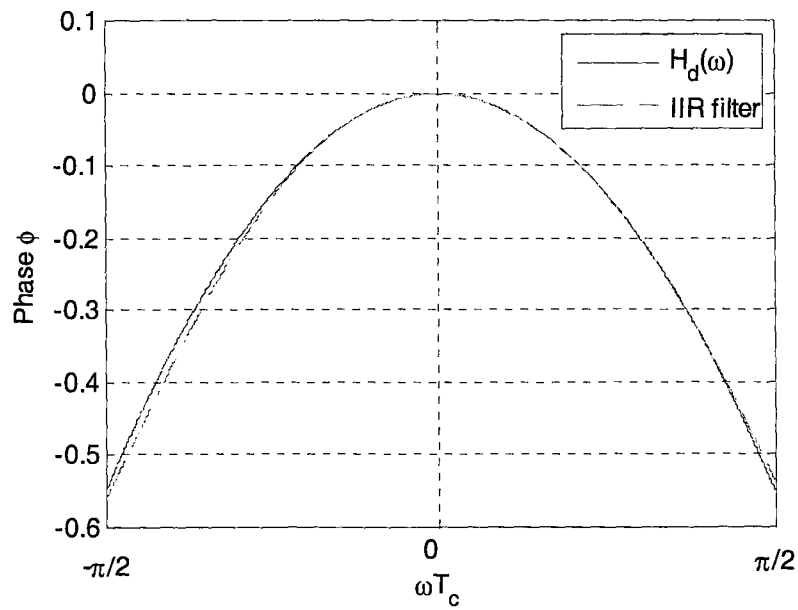

Figure 4.2 Phase

According to the description in the previous paragraphs, the computational complexity of this digital IIR filter is evaluated with a length $2(p+1)=4$, far smaller than the length of FIR filter. In each step, for dispersion part we only need do 3 multiplications and 2 additions, totally 5 operations. Though we have to reduce the step size to satisfy the requirement of this IIR filter design, this IIR filter is still much more efficient.

4.2 Implementation

4.2.1 Step Size Selection

In the split-step frequency domain method, only error introduced by the split-step is needed to be considered, because there is no error introduced in frequency domain linear propagation. Obviously, this split-step error can be controlled through the selection of Δz, the step size along the propagation direction. By introducing the second order dispersion length L_{D2}, the third order dispersion length L_{D3} and the nonlinear length L_{NL} defined as

$$L_{D2}=\frac{T_0^2}{\beta_2} \quad (4.17)$$

$$L_{D3}=\frac{T_0^3}{\beta_3} \quad (4.18)$$

$$L_{NL}=\frac{1}{\gamma e^{-\alpha z}P} \quad (4.19)$$

with T_0 indicating the input pulse width and P the peak power of the incident pulse. Δz must be selected as a fraction of the smallest of the above lengths.

In this split-step digital filtering approach, however, additional error (χ^2 in FIR and ε in IIR) has been introduced in the extraction of the digital filter. Therefore, further constraint on the step size may exist and should be analyzed. Generally, it is impossible to obtain such a fit in the phase over the entire frequency range with only limited terms. Letting W_p be the maximum range in phase in which the fitting error does not exceed ε and by ignoring the third order dispersion term, we have

$$\beta_2 \Delta z \omega^2 / 2 \le W_p \quad (4.20)$$

Noting that the time domain sampling interval Δ must satisfy $\Delta = 1/W_\omega$ with W_ω indicating the frequency domain window size (maximum ω), we obtain

$$\Delta z \le 2W_p \Delta^2 / \beta_2 \quad (4.21)$$

As W_p is normally in the range of a few phase periods (2π), we immediately find that the step size set by (4.21) is smaller than that given in (4.17) since $\Delta << T_0$. Similar analysis also applies when only 3rd order dispersion term is considered, where we have

$$\Delta z \le 2W_p\Delta^3 / \beta_3 \quad (4.22)$$

Again, this step size (4.22) is smaller than that given in (4.18). Thus, in digital filter algorithm, the step size must be chosen as the smallest of those given in equations (4.21), (4.22) and (4.19). This drawback is naturally brought into by the extra error introduced in linear propagation as an additional fitting must be introduced in the digital filter approach. The shrinkage on the required step size solely depends on the fitting quality: when a better fitting is achieved, W_p must be larger and the shrinkage will be smaller. As long as a fitting will make $W_p > (T_0^3 / \Delta^3)/2$, there is no extra constraint on the step size so that we can select the same step size as in the split-step frequency domain method. However, an enlarged W_p will inevitably lead to a lengthened filter that will again increase the computation cost. Therefore, there must be an optimized W_p in terms of the computation cost, which compromises the selections on the filter length and the step size.

In the digital filter algorithm, the accuracy is ensured by monitoring the conserved quantity in propagation, i.e., the pulse energy. Taking its maximum allowed quantity defined by equations (4.21), (4.22) and (4.19) as the initial value, the step size will automatically be reduced and the computation repeats if the variation of pulse energy is found to be beyond a predetermined small range.

For the IIR filter design described in this Chapter, the selection of Δz must satisfy another requirement. For the second order dispersion IIR filter, (4.7) must be equal to the linear term in (4.10), then we can get

$$\Delta z = 4\Delta^2 \frac{p_i\left(1-P_i^2\right)}{\beta_2\left(1+p_i^2\right)^2} \quad (4.23)$$

4.2.2 Validation of IIR Filter

Here, we will use this split-step IIR filtering approach to simulate the pulse propagation in fiber. In this simulation, only the negative second-order dispersion in

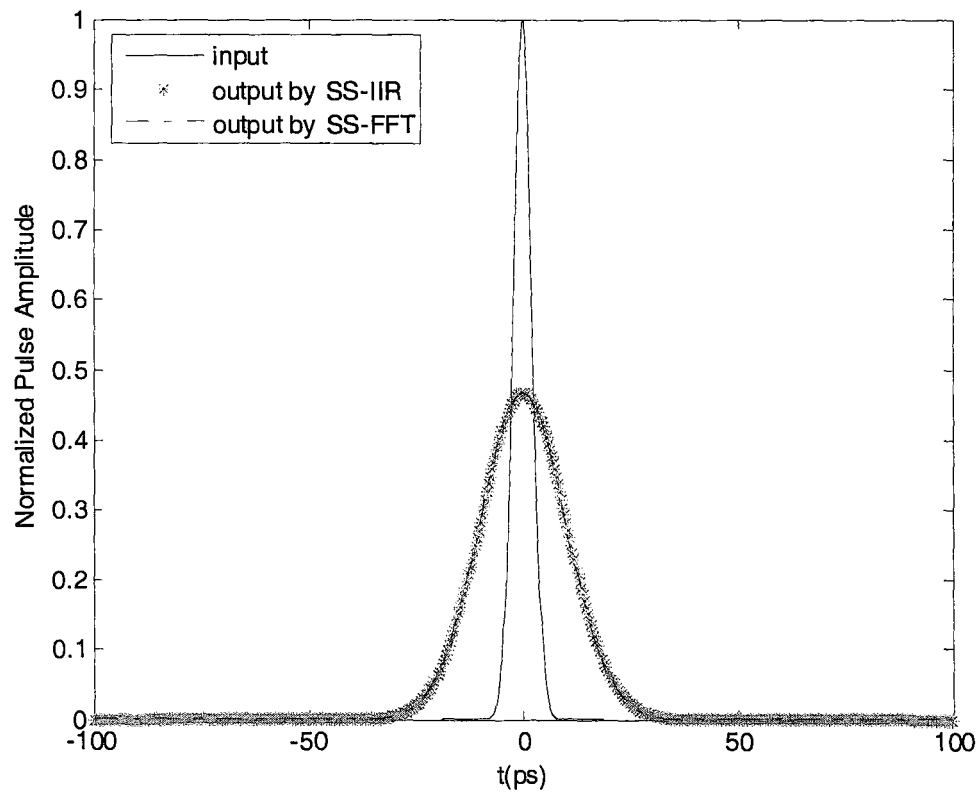

Figure 4.3 Gaussian pulse output after 150 steps

standard single mode fiber (SMF) is considered: $\beta_2 = -22\, ps^2/km$, $\beta_3 = 0$ with operating wavelength positioned at the center of the C-band ($1555.12nm$). No fiber nonlinearity is assumed ($\gamma = 0$).

To test the pulse propagation, a Gaussian input pulse is assumed with a width (T_0) of $3.125ps$. The time domain sampling interval is chosen as $\Delta = 0.390625ps$. To satisfy the requirement of this IIR filter design, we calculate to get $\Delta z = 0.0062km$. The results of pulse propagation are shown in figure 4.3, from which we can see the exact agreement between the two approaches.

Chapter 5

Split-step IIR-DSP Method for CNSE

Compared with split-step FIR DSP approach for CNSE, split-step IIR filtering method uses IIR filter to replace the FIR filter to treat the linear propagation part, while the way to treat nonlinearity part stays the same. Because of this replacement, computation time and memory size will be saved greatly.

The split-step IIR filtering algorithm in solving CNSE contains two main routines. In the first routine, we extract all the necessary filter coefficients for a given fiber. This routine only needs to be computed once for a given fiber. The second routine is to deal with each split-step. Assuming that we have K split-step, N subintervals for each split-step and L possible sample frequency domain transfer functions, a simple diagram is given in figure 5.1.

In the first routine, the following steps will be taken to extract IIR filter coefficients:

Step 1: A random code generator (RCG), defined by a Gaussian random process, will be called to generate L status. This set of status will be used to compute the random birefringence orientations.

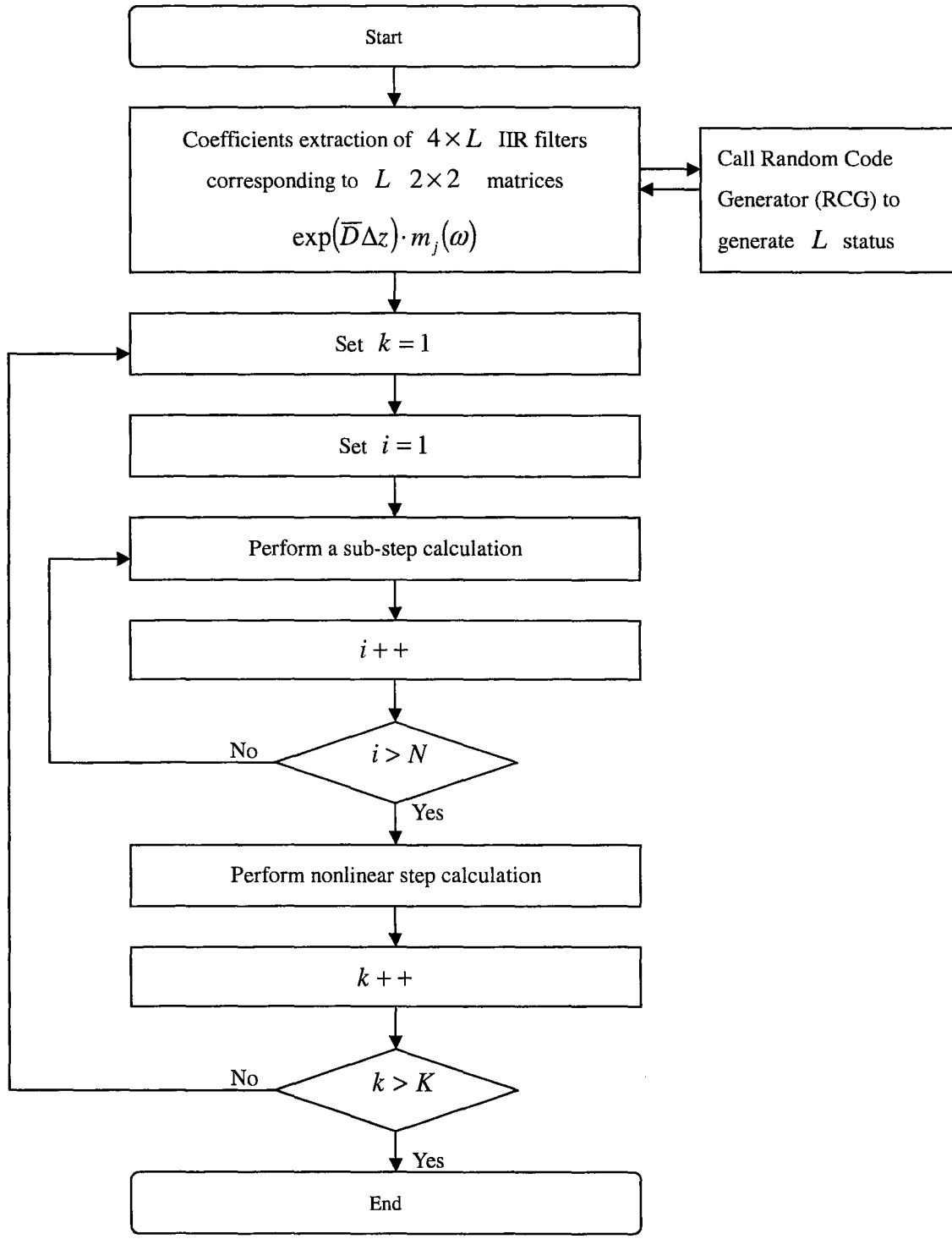

Figure 5.1 Diagram of time domain IIR filtering approach for CNSE

Step 2: Compute all 2×2 matrices $\exp(\overline{D}\Delta z)\cdot m_l, l=1,2,3,\ldots L$, corresponding to the L status of θ_l.

Step 3: Corresponding to the four elements in each $\exp(\overline{D}\Delta z)\cdot m_l(\omega)$ matrix, extract the four IIR filters. Obtain all L different 2×2 IIR filter matrices. Store them as $A^l, l=1,2,\ldots,L$.

In the second routine, we will perform each split-step. For each split-step Δz, we further divide it into N subsections with the same length. As described in Chapter 2, the birefringence orientation varies randomly from subsection to subsection while the birefringence strength is fixed. $\delta z=\frac{\Delta z}{N}$ and $N=500$ is chosen, and it is enough to cover the randomness of the birefringence. The time domain signal will pass through these N IIR filter matrices, which account for the random rotation of the birefringence effects and dispersion.

For the i^{th} subsection,

$$U_1^{i\delta z(T)}=\left(\sum_{k=0}^{P}a_{l,k}^{11}U_1^{(i-1)\delta z(T-k\Delta)}-\sum_{k=1}^{P}b_{l,k}^{11}U_1^{i\delta z(T-k\Delta)}\right)+\left(\sum_{k=0}^{P}a_{l,k}^{12}U_2^{(i-1)\delta z(T-k\Delta)}-\sum_{k=1}^{P}b_{l,k}^{12}U_2^{i\delta z(T-k\Delta)}\right)$$
$$U_2^{i\delta z(T)}=\left(\sum_{k=0}^{P}a_{l,k}^{21}U_1^{(i-1)\delta z(T-k\Delta)}-\sum_{k=1}^{P}b_{l,k}^{21}U_1^{i\delta z(T-k\Delta)}\right)+\left(\sum_{k=0}^{P}a_{l,k}^{22}U_2^{(i-1)\delta z(T-k\Delta)}-\sum_{k=1}^{P}b_{l,k}^{22}U_2^{i\delta z(T-k\Delta)}\right)$$

(5.1)

This operation is defined as

$$U^{i\delta z} = A_l U^{(i-1)\delta z} \quad (5.2)$$

where l is a number from 1 to L randomly selected by a random code generator (RCG).

For k^{th} split-step Δz, we will perform the following two steps: linear step and nonlinear step. The diagram is shown in figure 5.2:

Step 1: According to the RCG assigned number $k1$ (a number in the range from 1 to L), pick

$$A_l = A_{k1}$$

as the first IIR filter matrix for the first subsection $i = 1$ and perform:

$$U^{\delta z} = A_{k1} U^0$$

Then according to the RCG assigned number $k2$, pick $A_l = A_{k2}$ as the second IIR filter matrix for subsection $i = 2$ and perform $U^{2\delta z} = A_{k2} U^{\delta z}$. Similarly, for each subsection from $i = 3$ to $N-1$, pick IIR filter matrix according to the RCG assigned number, $k3$ to $k(N-1)$. Finally, get the RCG assigned number kN, pick $A_l = A_{kN}$ as the last IIR

filter matrix for the last subsection $i = N$ and perform $U^{N\delta z} = A_{kN}U^{(N-1)\delta z}$.

All together for k^{th} split-step Δz, this process can be expressed as

$$\overline{U}^{\Delta z} = A_{kN}A_{k(N-1)}A_{k(N-2)}\cdots A_{k1}U^0 \quad (5.3)$$

Step 2: we will deal with nonlinear part to complete k^{th} split-step Δz,

$$\begin{aligned} U_1(z+\Delta z,T) &= \exp(\Delta z N_1)\overline{U}_1(z+\Delta z,T) \\ U_2(z+\Delta z,T) &= \exp(\Delta z N_2)\overline{U}_2(z+\Delta z,T) \end{aligned} \quad (5.4)$$

To summarize, in a total split-step length Δz, input signal will firstly pass through N IIR filter matrices selected by randomly picking out one of the L pre-determined IIR filter matrices at each subsection δz, Then pass through the nonlinear part. Thus, we move one split-step Δz forward. Because we have total number of K Δz step, then we will perform the split-step procedure for K times.

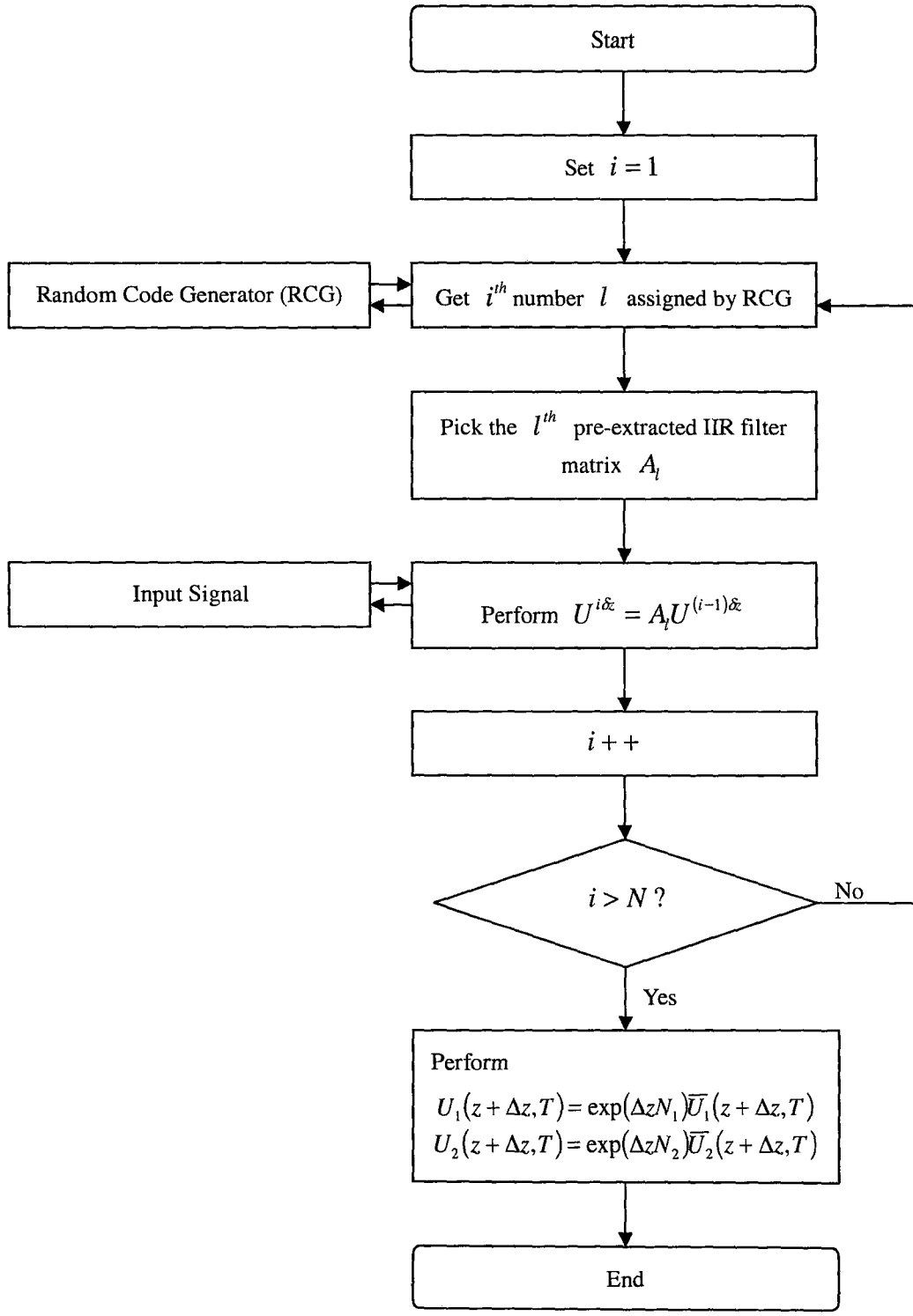

Figure 5.2 Diagram for each split-step

Chapter 6

Implementation of Split-step IIR filtering Approach for CNSE

In this section, we will validate our algorithm through comparison between the traditional frequency domains split-step Fourier method and the time domain split-step IIR filtering method in optical pulse propagation when considering PMD effects. We will show that the simulation using the proposed IIR filtering method leads to precisely the same result as is obtained by conventional split-step Fourier approach. Five cases have been chosen to demonstrate the simulations results. All computations reported here were run without fiber loss and it will not affect the generality of our analyses.

6.1 Wide Gaussian Input Pulse

We selected the following parameters: $\beta_2 = -21.6\, ps^2/km$ and $\beta_3 = 0$ with operating wavelength at the center of the C-band (1555.12nm). Parameters b and b' are selected as $b = 0.20268 m^{-1}$ and $b' = 6.708\, ps/(km \cdot m)^{\frac{1}{2}}$, [17]. The birefringence orientation rotates randomly from section to section, but the birefringence strength is assumed to be constant. The input power is distributed as 50:50 for fast axis and slow axis. The step size is selected as $\Delta z = 1km$. The time domain sampling interval is selected as $\Delta = 4.9238 ps$, a Gaussian input pulse is assumed with a width $T_0 = 50 ps$.

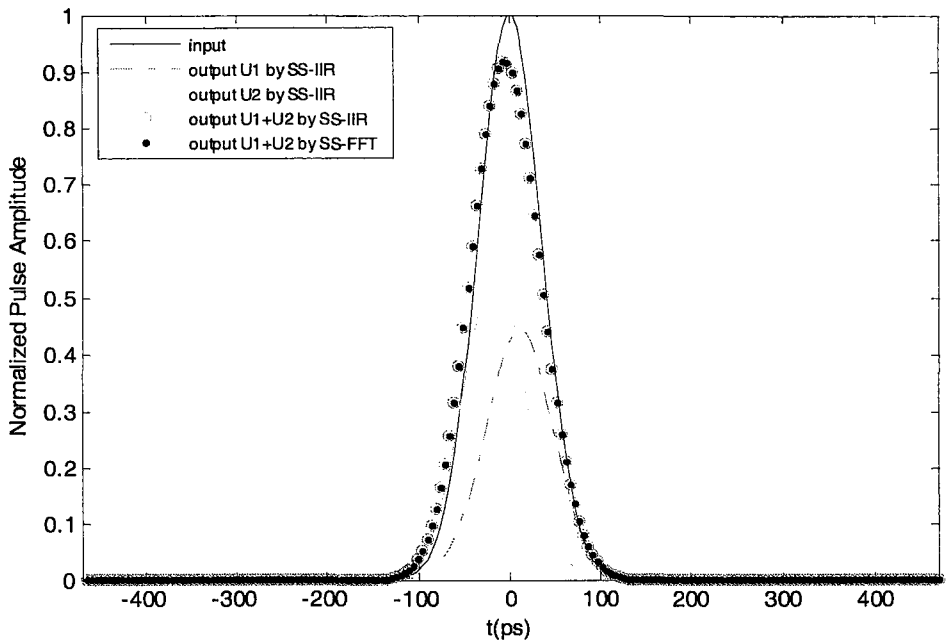

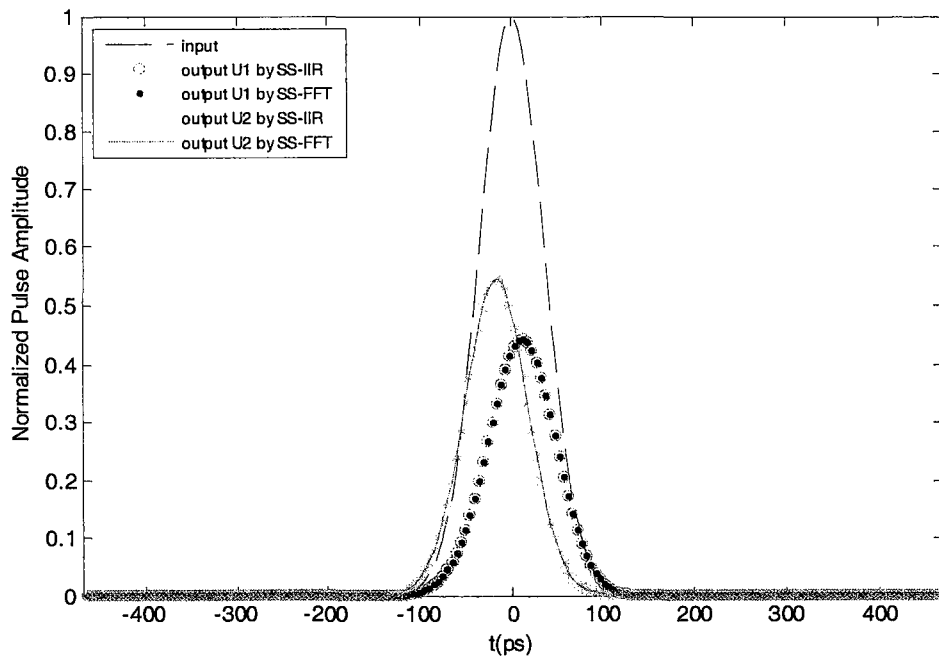

(a) after 4 steps, $\Delta z = 1km$

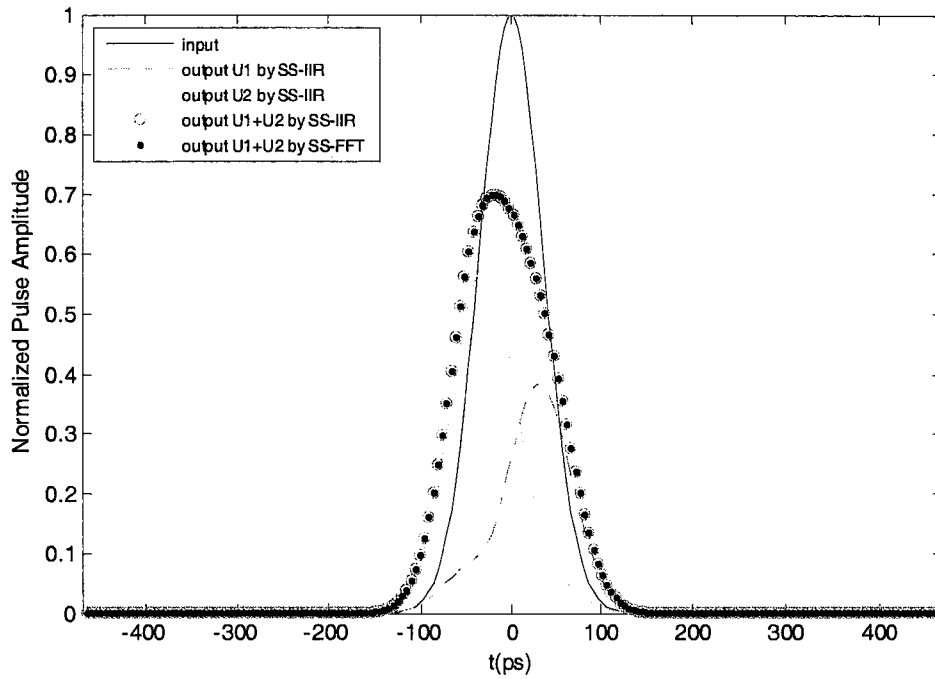

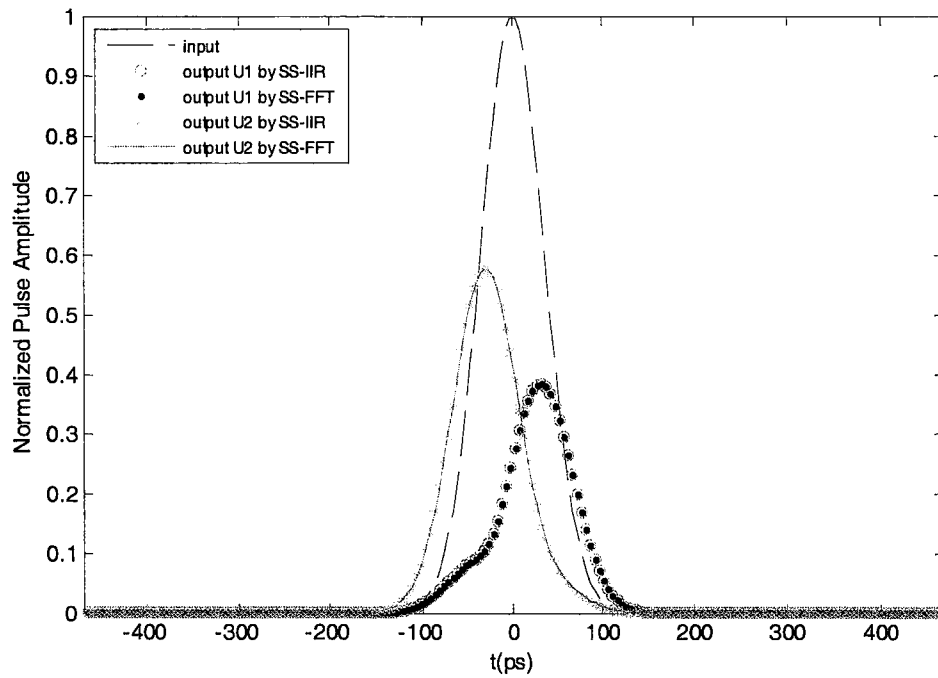

(b) after 8 steps, $\Delta z = 1km$

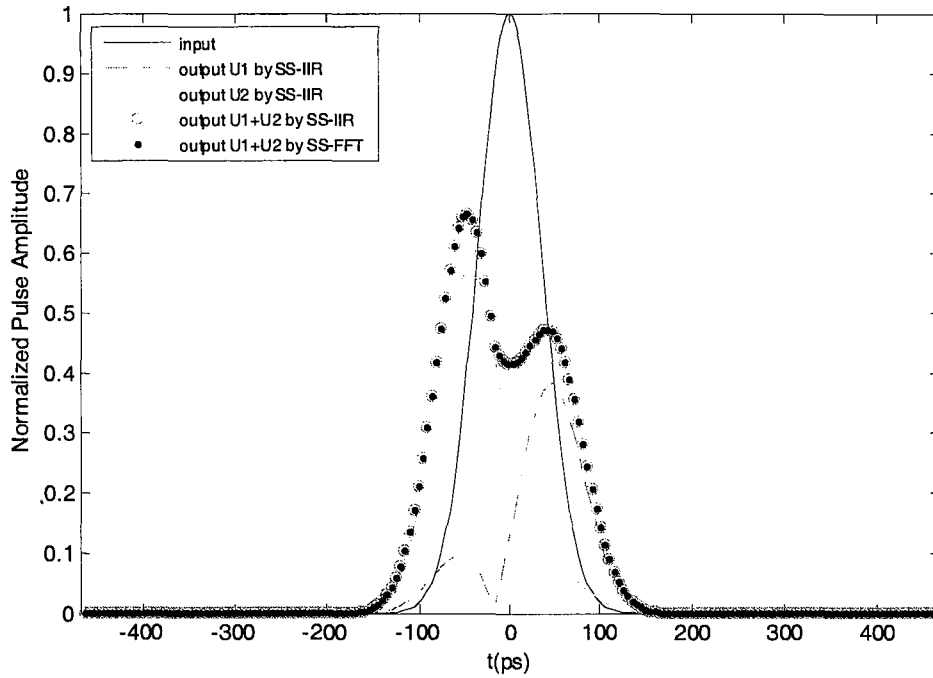

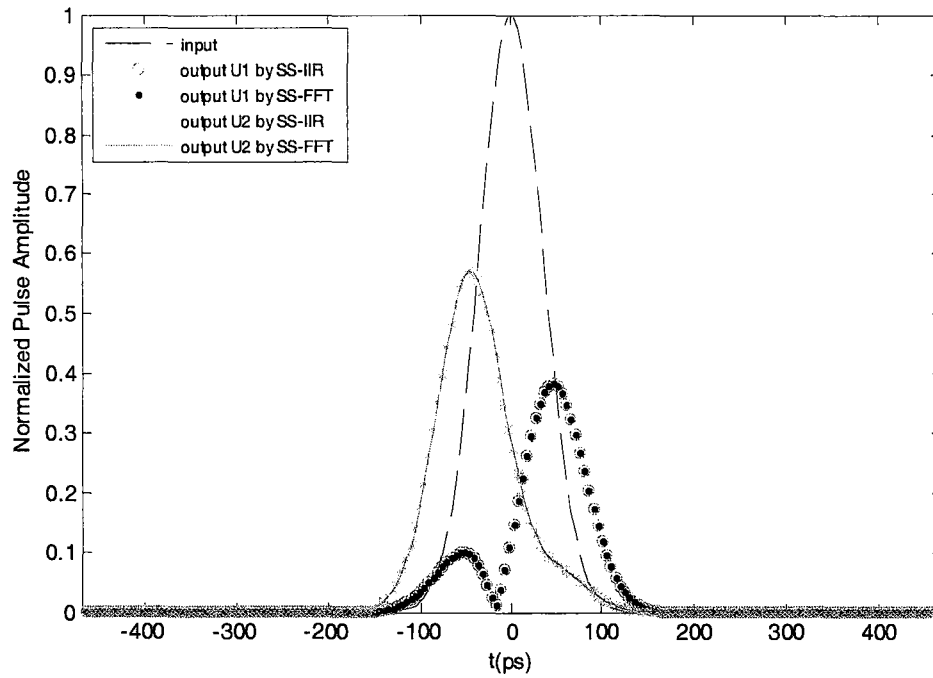

(c) after 12 steps, $\Delta z = 1km$

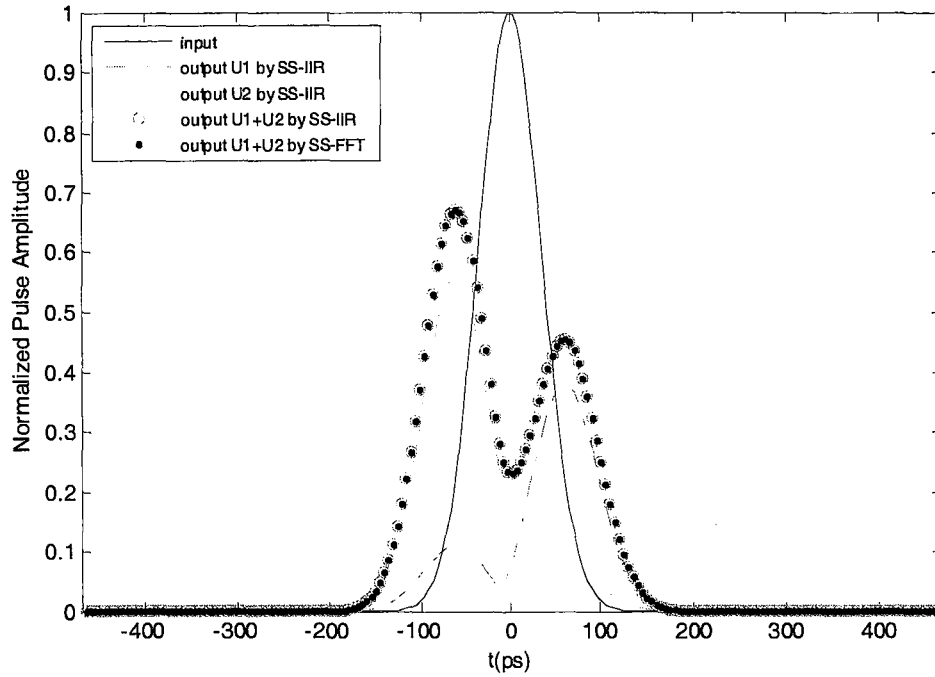

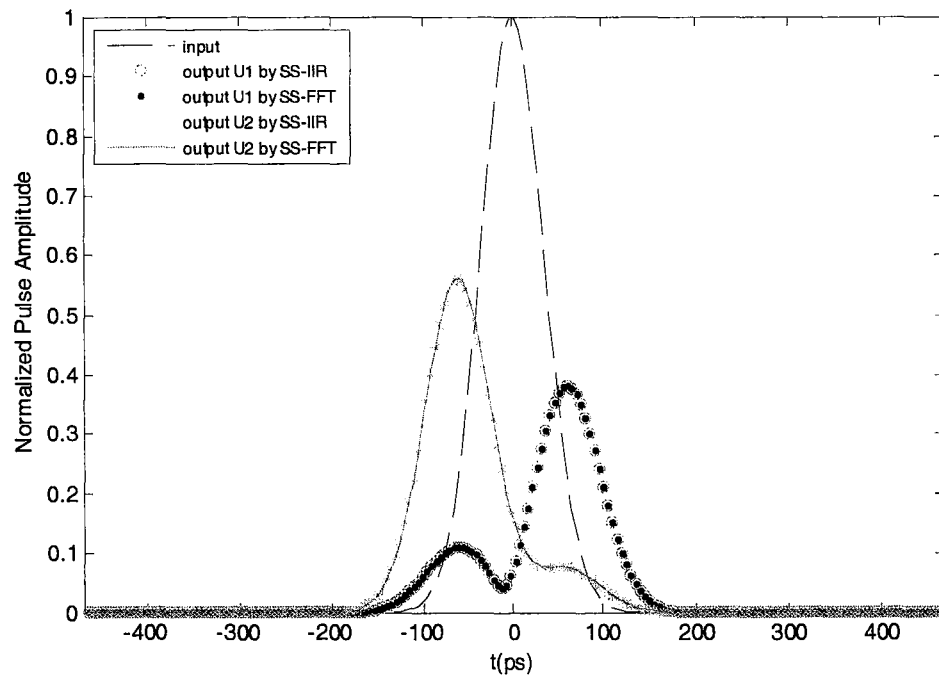

(d) after 16 steps, $\Delta z = 1km$

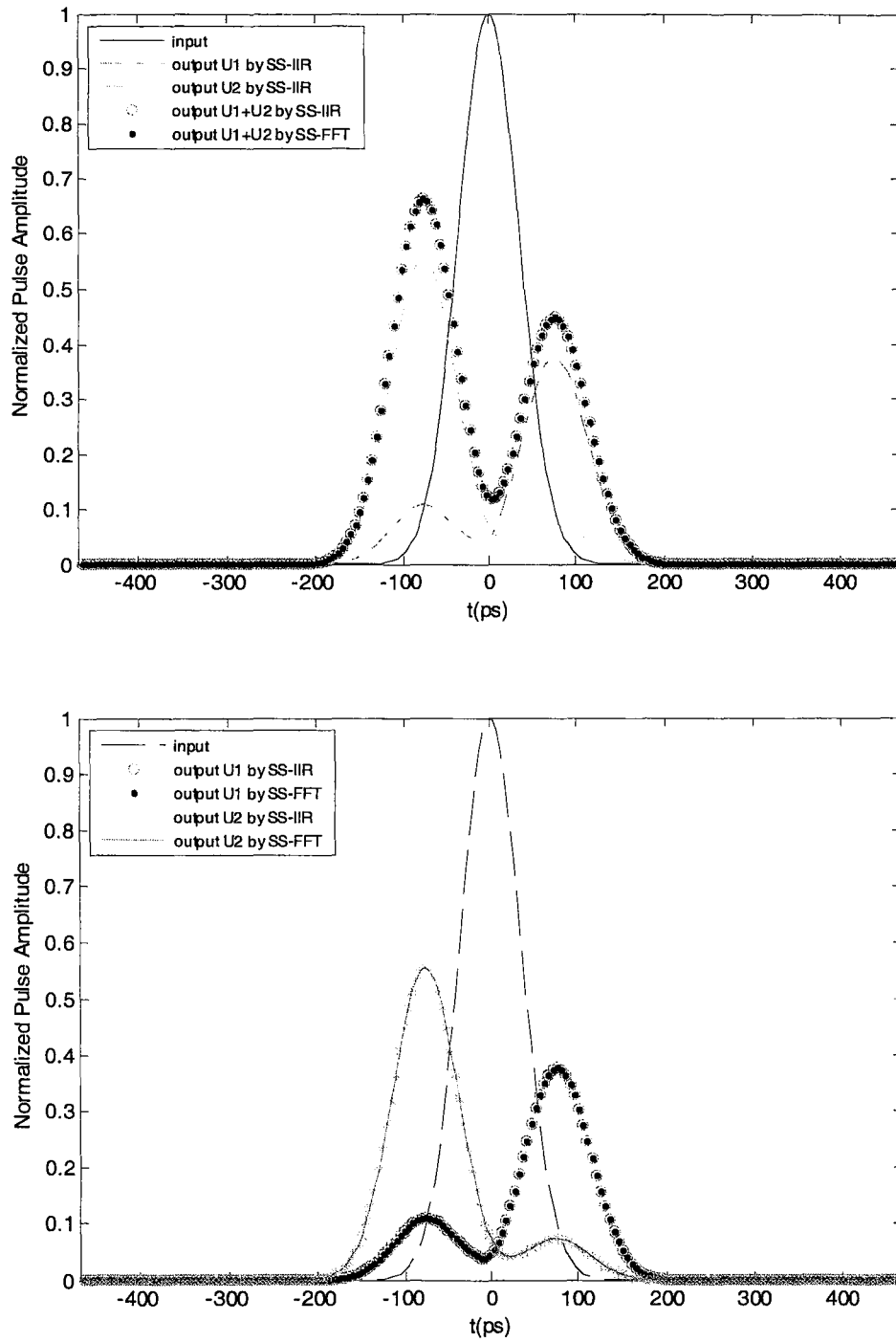

(e) after 20 steps, $\Delta z = 1km$

Figure 6.1 Simulation results by split-step IIR filter method and FFT methods

The pulse propagation simulation results from split-step Fourier method and the split-step IIR method are showed in figure 6.1, where $U1$ and $U2$ are the outputs of fast axis and slow axis, respectively. These two approaches produce exactly the same results for the same assumed variation of the fiber birefringence. But we found that the shape of the distorted pulses is strongly dependent on the random number sequence used for computing the random variation of the birefringence orientation angles. This dependence corresponds physically to the observation that different fibers with different random variations of the birefringence will have somewhat different behaviors. To solve this problem, we can implement the simulation with all possible random number sequences, and then get the average results.

6.2 Wide Gaussian Pulse Propagation in Fiber with Stronger PMD

In the second simulation, we selected the following parameters: $\beta_2 = -21.6\, ps^2/km$ and $\beta_3 = 0$, $b = 0.20268 m^{-1}$ and $b' = 15.811\, ps/(km \cdot m)^{\frac{1}{2}}$. In this test, the peak of the input pulse is again normalized to 1 and the input power is distributed as 50:50 for fast axis and slow axis. $\Delta z = 1km$ is selected as the step size. Time domain sampling interval is selected as $\Delta = 4.9238 ps$. Gaussian input pulse is assumed with a width $T_0 = 50 ps$.

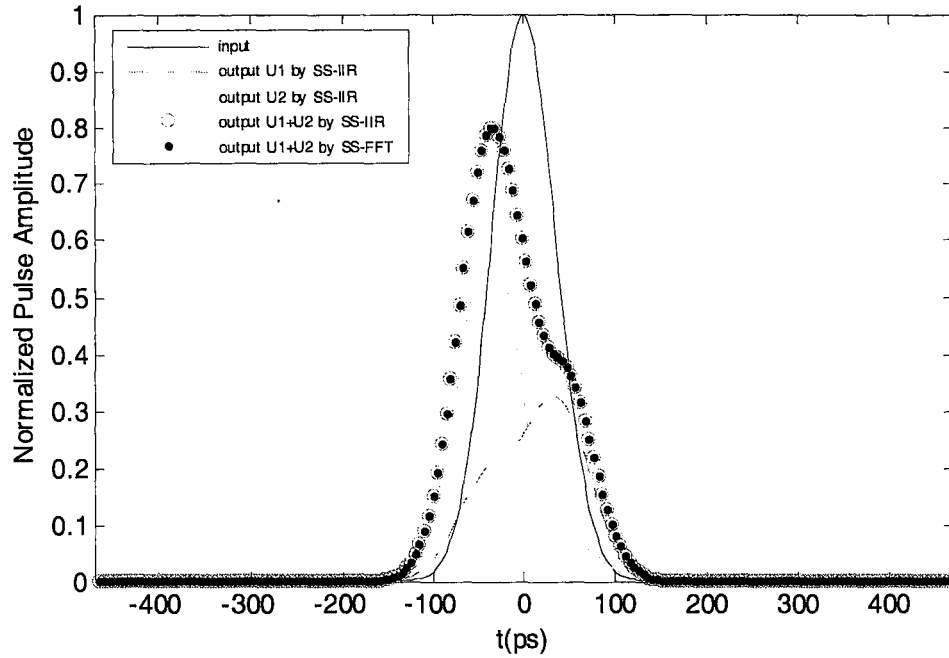

(a) after 4 steps, $\Delta z = 1km$

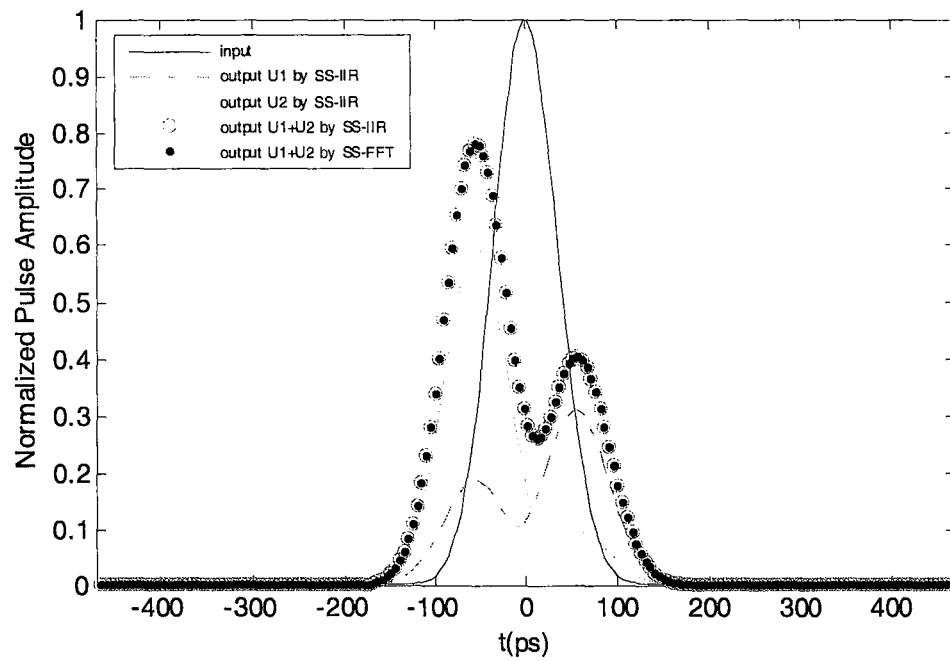

(b) after 6 steps, $\Delta z = 1km$

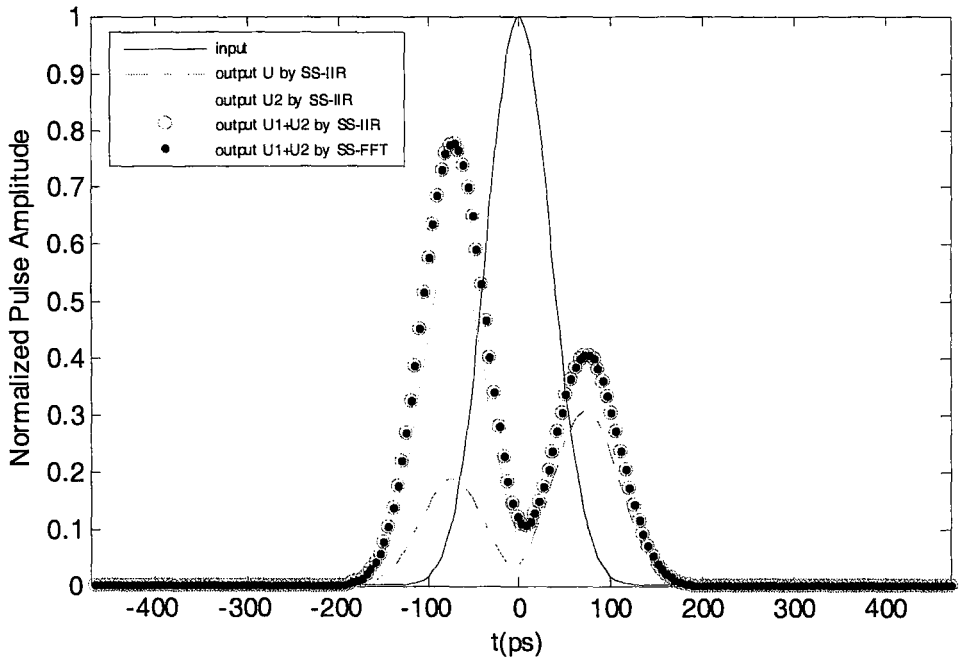

(c) after 8 steps, $\Delta z = 1km$

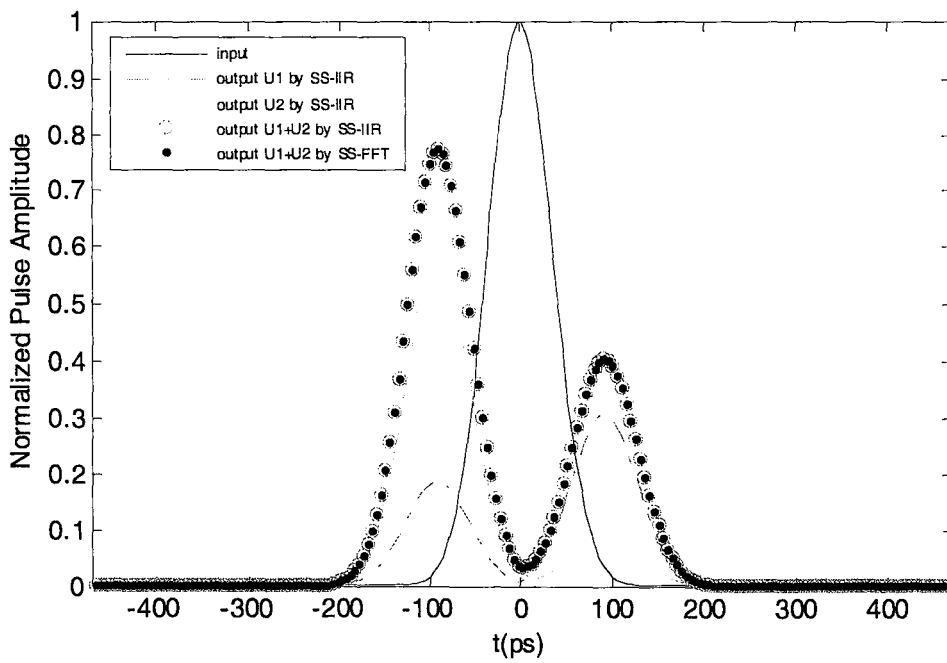

(d) after 10 steps, $\Delta z = 1km$

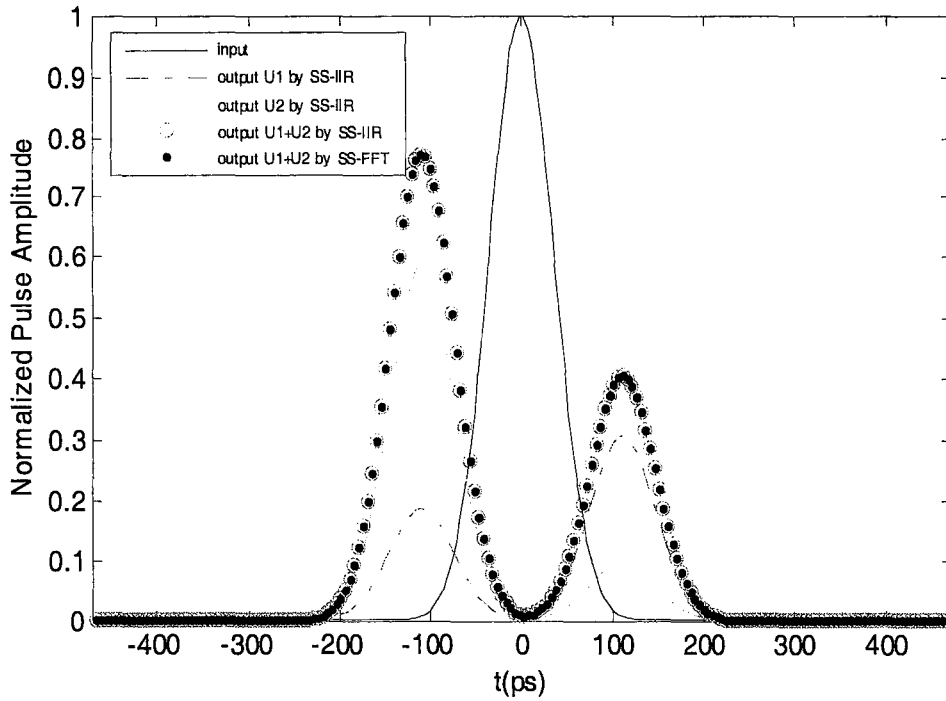

(e) after 12 steps, $\Delta z = 1km$

Figure 6.2 Simulation results by split-step IIR filter method and FFT methods

The simulations results are shown in figure 6.2. This time we still get exact agreement between the results from these two different approaches. Compared with the simulation results in 6.1, we found that larger b', which means stronger PMD, can lead to more severe pulse distortion in propagation.

6.3 Wide Gaussian Pulse Propagation in Fiber with Smaller Birefringence

In the third simulation, we selected the following parameters: $\beta_2 = -21.6\, ps^2/km$ and $\beta_3 = 0$, $b = 6.2831\times10^{-2} m^{-1}$ and $b' = 15.811\, ps/(km\cdot m)^{\frac{1}{2}}$. The peak of the input pulse is again normalized to 1 and $\Delta z = 1km$ is selected as the step size. Time domain sampling interval is selected as $\Delta = 4.9238 ps$. Gaussian input pulse is assumed with a width $T_0 = 50 ps$.

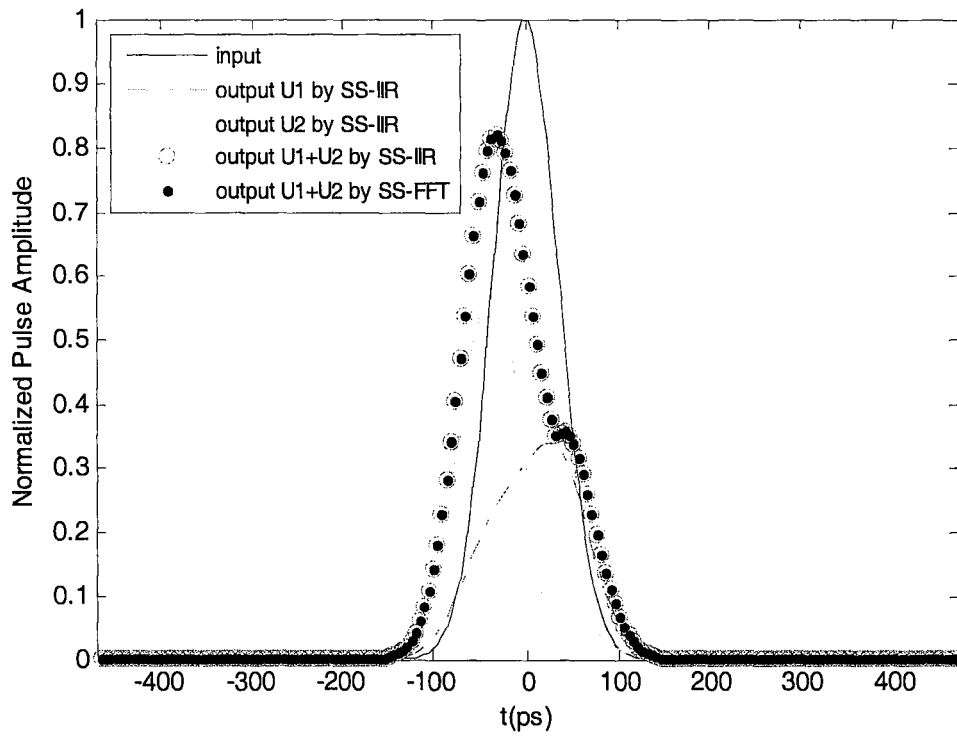

(a) after 4 steps, $\Delta z = 1km$

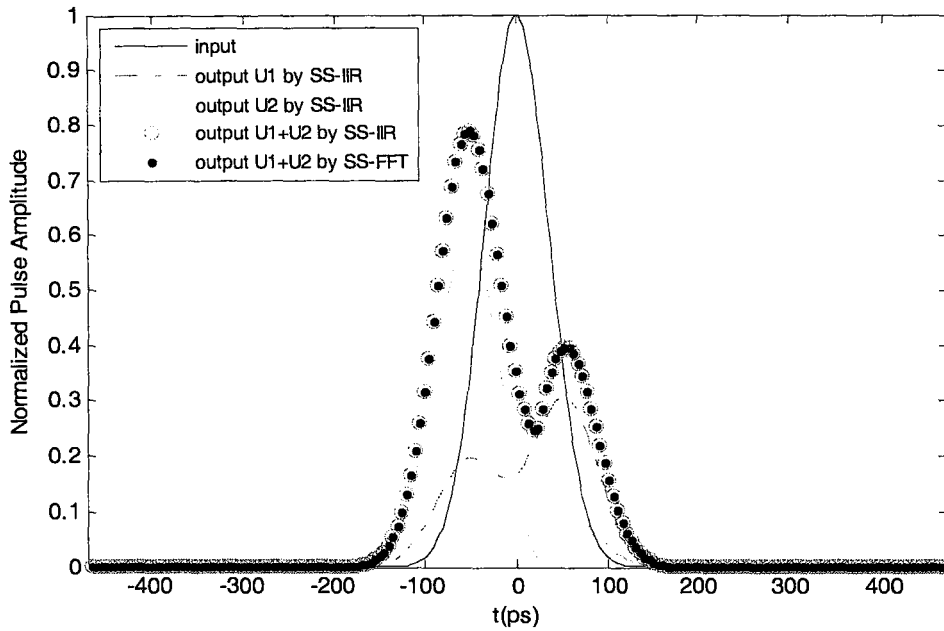

(b) after 6 steps, $\Delta z = 1km$

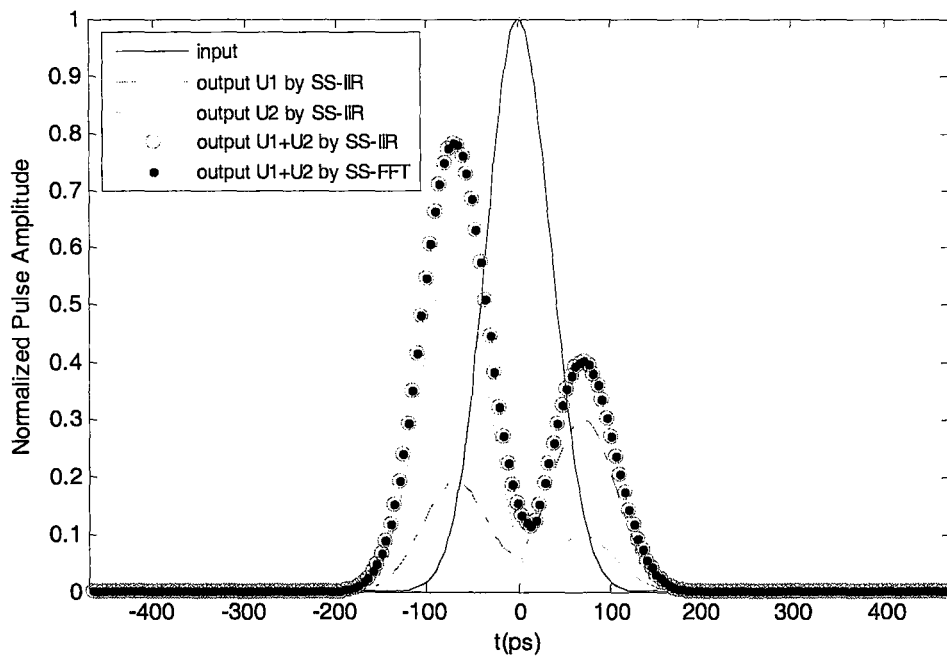

(c) after 8 steps, $\Delta z = 1km$

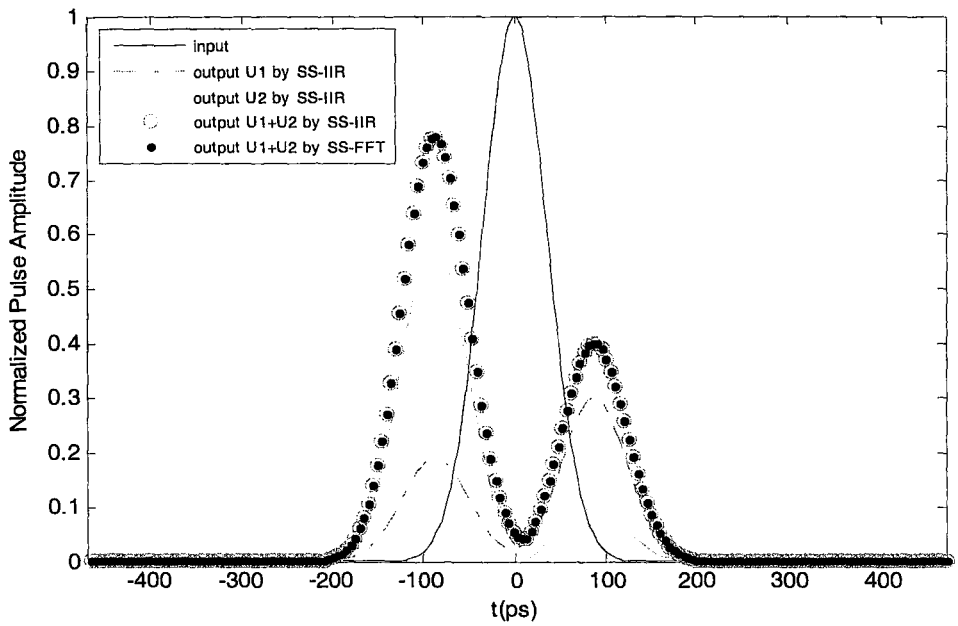

(d) after 10 steps, $\Delta z = 1km$

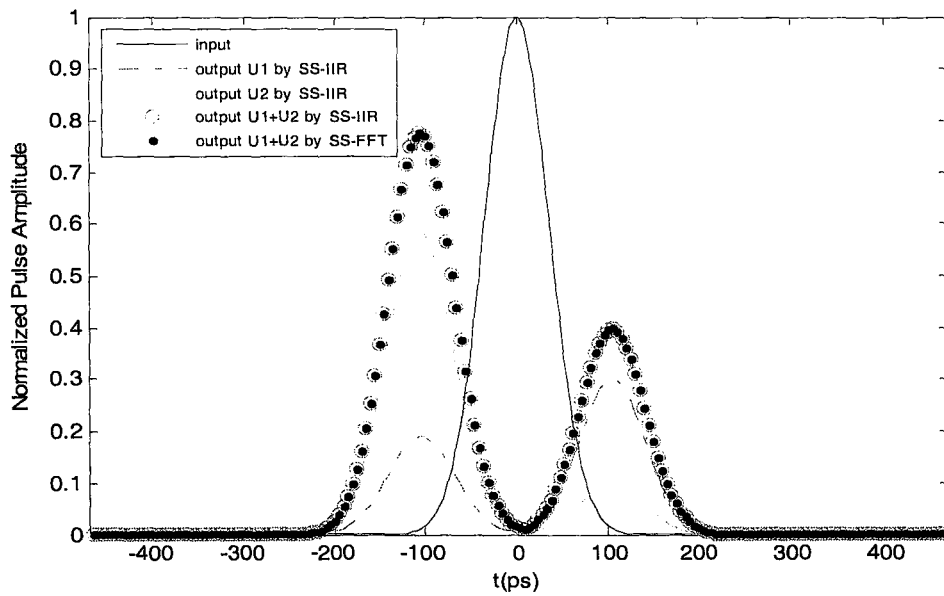

(e) after 12 steps, $\Delta z = 1km$

Figure 6.3 Simulation results by split-step IIR filter method and FFT methods

Figure 6.3 still show exact agreement between the two approaches. Compared with the results in 6.2, we found that different b would not produce obvious difference on the shape of the output pulse. But smaller b, which means smaller birefringence, will make the power between the slow mode and fast mode exchange more slowly as they propagate in the fiber.

6.4 Narrow Gaussian Input Pulse

In the fourth simulation, we study a narrow Gaussian pulse with a width of $T_0 = 5ps$. The peak of the input pulse is again normalized to 1, and time domain sampling interval is selected as $\Delta = 0.3482ps$. A smaller step size $\Delta z = 0.005km$ is selected. We use the following parameters: $\beta_2 = -21.6\, ps^2/km$ and $\beta_3 = 0$, $b = 6.2831 \times 10^{-2} m^{-1}$ and $b' = 15.811\, ps/(km \cdot m)^{\frac{1}{2}}$.

Figure 6.4 show the narrow Gaussian pulse propagation simulation results. With split-step IIR filtering method we still get the same result as the split-step FFT approach does. But we found that the output pulse is deformed more severely after only couple kilometers of propagation because PMD has a stronger effect on narrow Gaussian pulse.

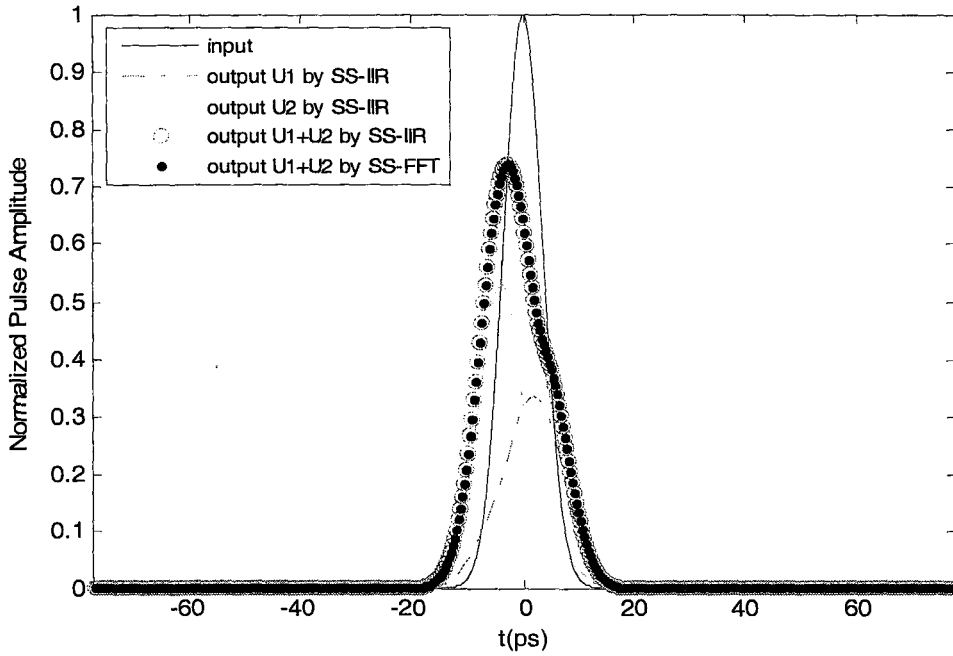

(a) after 80 steps, $\Delta z = 0.005km$

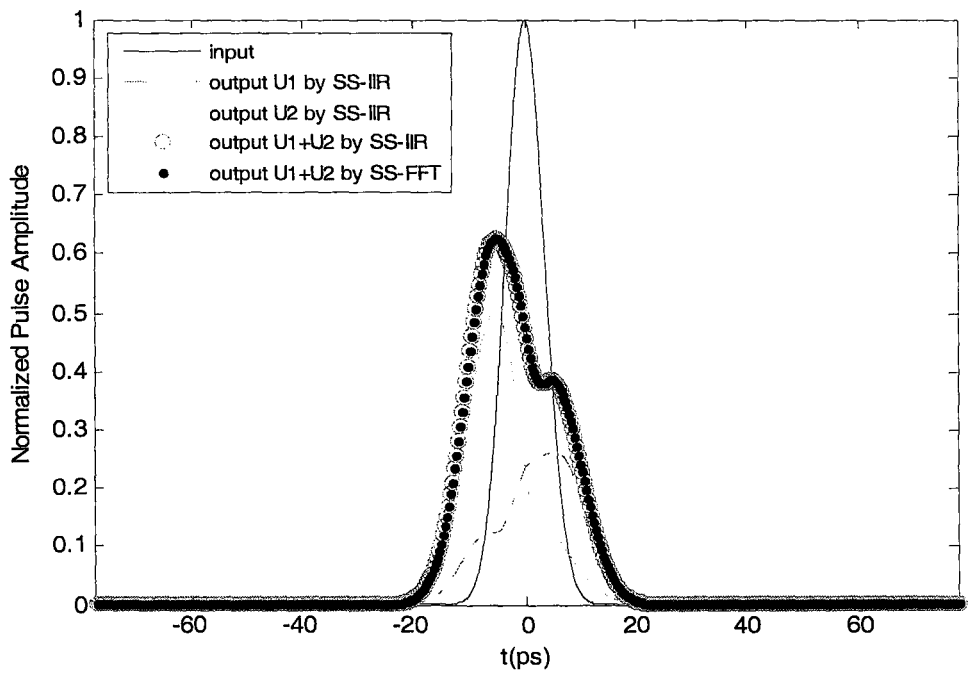

(b) after 120 steps, $\Delta z = 0.005km$

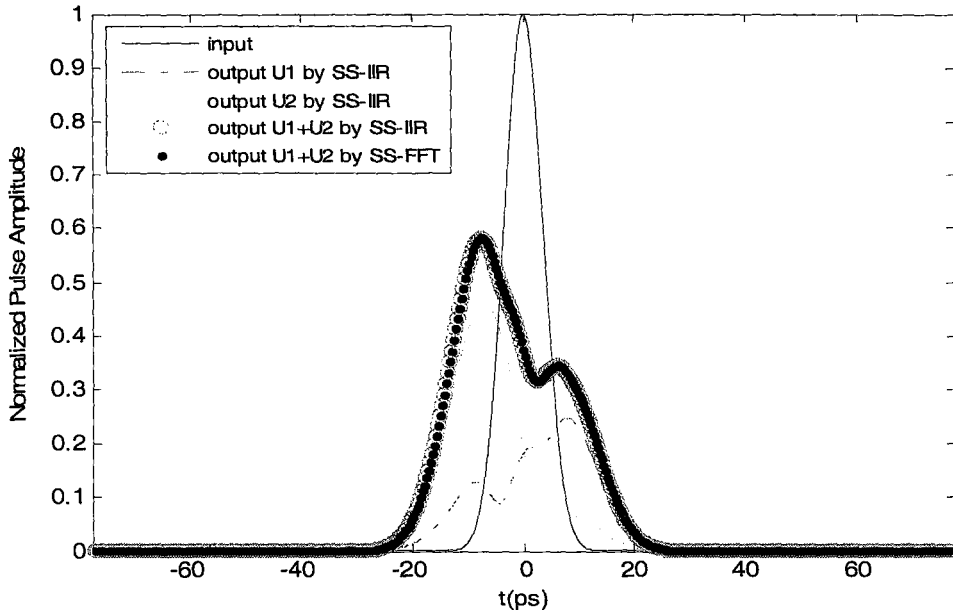

(c) after 160 steps, $\Delta z = 0.005km$

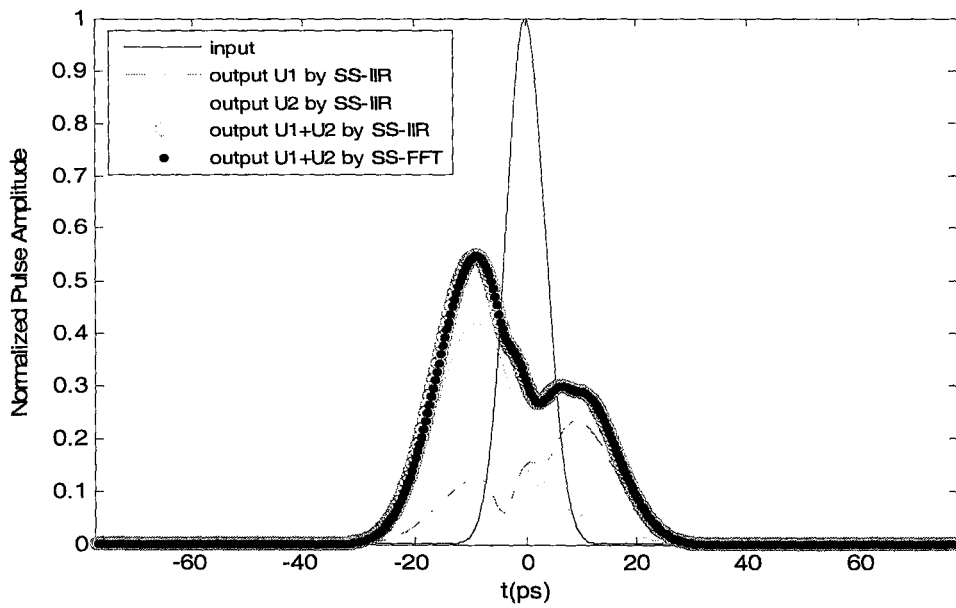

(d) after 200 steps, $\Delta z = 0.005km$

Figure 6.4 Simulation results by split-step IIR filter method and FFT method

6.5 Gaussian Pulse Propagation in Dispersion-Shifted Fiber

In the fifth simulation, we study PMD effect on dispersion compensation. We simulated the pulse propagation in a fiber span which is made up of a $150km$ stretch of dispersion-shifted fiber with $\beta_2 = 2ps^2/km$, followed by a $15km$ stretch of conventional fiber with $\beta_2 = -20ps^2/km$. A birefringence average beat length of $50m$ is chosen, together with a PMD value of $3ps/\sqrt{km}$. The birefringence correlation length is assumed to be $100m$. In this test, the peak of the input pulse is again normalized to 1 and $\Delta z = 1km$ is selected as the step size in dispersion-shifted fiber, $\Delta z = 0.1km$ in conventional fiber. Time domain sampling interval is selected as $\Delta = 1.4983ps$. Gaussian input pulse is assumed with a width $T_0 = 25ps$.

Figure 6.5 show the pulse propagation simulation results from split-step Fourier method and the split-step IIR method. The output pulses calculated by different algorithm are still exactly identical. Figure 6.6 show the pulse propagation simulation results without PMD effect. By comparing figure 6.5 and 6.6, we can find that, due to PMD effect, pulse propagation cannot be well dispersion-compensated.

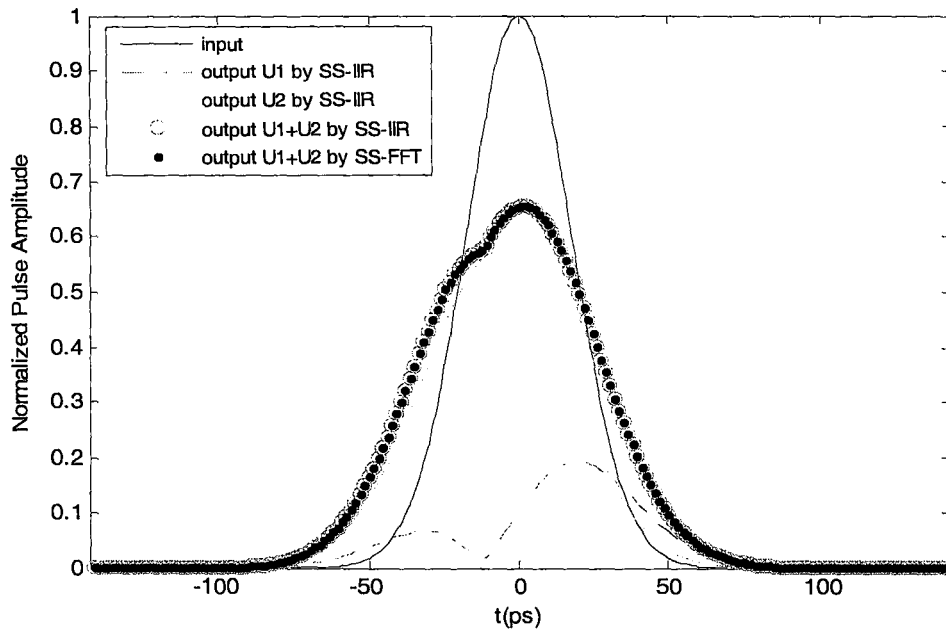

(a) Pulse propagation in dispersion-shifted fiber (After 150 steps, step size is $1km$)

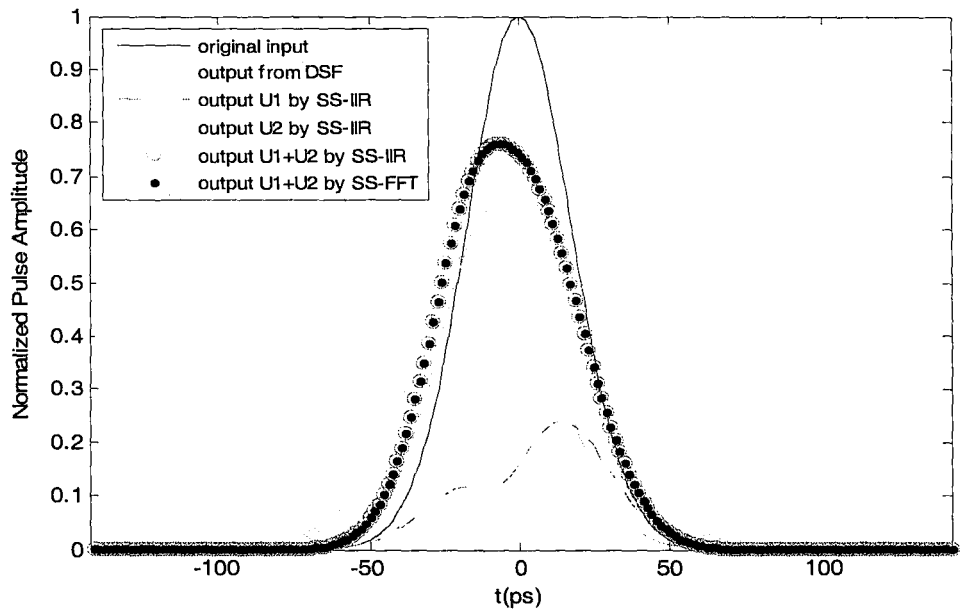

(b) Pulse propagation in conventional fiber (After 150 steps, step size is $0.1km$)

Figure 6.5 Simulation results by split-step IIR filter method and FFT methods

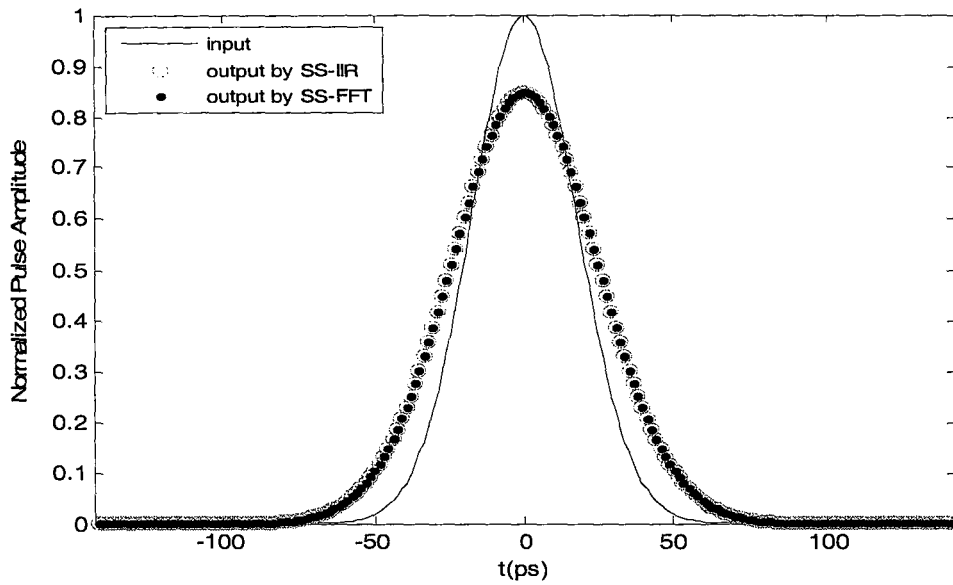

(a) Pulse propagation in dispersion-shifted fiber (After 150 steps, step size is $1km$)

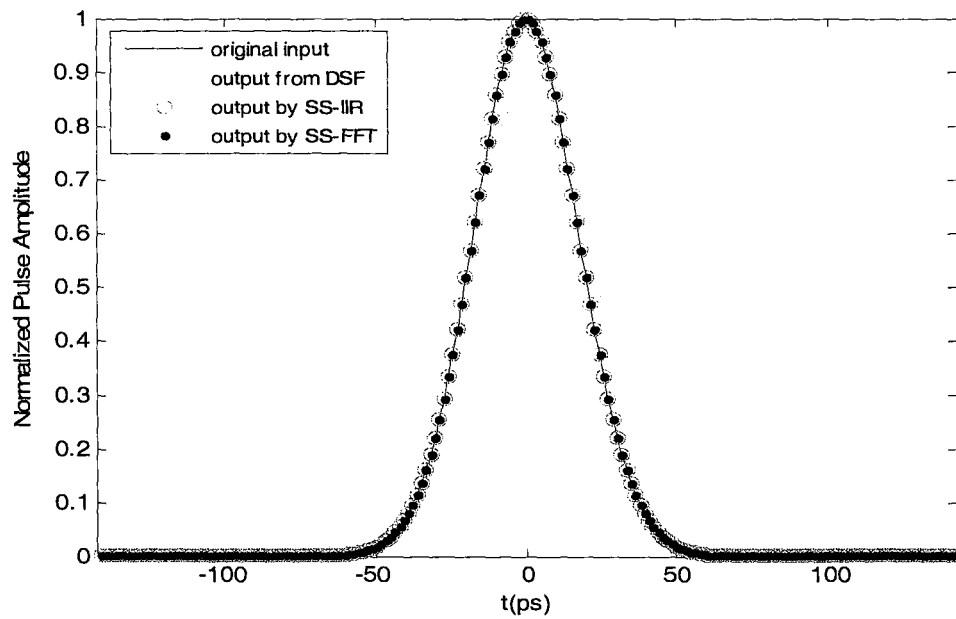

(b) Pulse propagation in conventional fiber (After 150 steps, step size is $0.1km$)

Figure 6.6 Simulation results by split-step IIR filter method and FFT methods

Chapter 7

Conclusions

7.1 Conclusions

In this thesis, a time domain split-step IIR filtering approach is proposed and implemented for the simulation of light pulse propagation in fiber with PMD effects considered. We reviewed the frequency domain split-step Fourier method and time domain FIR filtering method. We applied this time domain split-step IIR filtering approach to solve CNSE and several simulation examples are given.

Using the conventional split-step FFT method as the benchmark, we have validated the proposed approach and found that this time domain split-step IIR filtering approach can achieve exact agreement. As a full time domain simulator in optical fiber communication systems, this approach has outstanding advantages: it can be fully realized in a data-flow fashion; it makes the noise treatment much easier; it makes the distributed and parallel computing possible; it meets causality requirement automatically since the output signal sample will depend on the past input signal sample only; it is computationally less complex and can save much more computation time and memory size than time domain FIR filtering method.

In our simulation, each step Δz is divided into 500 subintervals. For each

subinterval, the computation complexity of split-step FIR filtering approach is $O(M^2) = O(512^2) = O(262144)$, while the computation complexity of split-step IIR filtering approach is only $O((2(P+1))^2) = O(16)$. It is very obvious that this IIR approach is much less computationally complex than FIR approach.

7.2 Future Works

The proposed time domain split-step IIR filtering method has been studied only for the second order dispersion. The design of IIR filter for the third order dispersion still needs to be studied in the future work.

References

[1] Ivan P. Kaminow and Thomas L. Koch, "*Optical Fiber Telecommunications III-A*", Academic Press, 1997.

[2] John M. Senior, "*Optical Fiber Communications, Principles and Practice*", 2nd edition, Prentice Hall, 1992.

[3] Marcello Potenza, "*Optical Fiber Amplifiers for Telecommunication Systems, IEEE Communications Magazine*", August 1996.

[4] A. Carena, V. Curri, R. Gaudino, P. Poggiolini, S. Benedetto, "*A Time-Domain Optical Transmission System Simulation Package Accounting for Nonliear and Polarization-Related Effects in Fiber*", IEEE J. Select. Areas Commun., Vol. 15, pp. 751-764, May 1997.

[5] N.Yajima and A. Outi, *Progress of Theoretical Physics*, vol. 45, pp. 1997, 1971.

[6] R.H. Hardin and F.D. Tappert, "*Applications of Split-step Fourier method to the Numerical Solution of Nonlinear and Variable Coefficient Wave Equation*," SIAM Rev. Chronicle, vol.15, pp. 423, 1973.

[7] R. A. Fisher and W.K. Bischel, "*The Role of Linear Dispersion in Plane-Wave Self-Phase Modulation*," Appl. Phys. Lett. 23, pp.661, 1973.

[8] I.S. Greig and J.L. Bischel, "*A hopscotch method for the Korteweg-de-Vries equation*," Journal of Computational Physics, vol. 20, pp.64-80, 1973.

[9] M. Delfour, M Fortin, and G. Payre, "*Finite-difference solutions of a non-linear Schrodinger equation*," J. Computational Physics, vol. 44, pp.277-288, 1981.

[10] L.R. Watkins and Y.R. Zhou, "*Modeling Propagation in Optical Fibers using Wavelet*," J. Lightwave Technol., vol. 12, pp.536-1542, Sept. 1994.

[11] X. Li, X. Chen, and M.S. Qasmi, "*A Broadband Digital Filtering Approach for Time Domain Simulation of Pulse Propagation in Optical Fiber*," OSA/IEEE Journal of Lightwave Technology, vol. 23, no. 2, pp. 864-875, Feb. 2005.

[12] Pak Kei Law, "*A Digital Filtering Approach for Simulation of Pulse Propagation over Optical Fiber with Polarization Mode Dispersion Effect*", Thesis, Mcmaster University, 2004.

[13] W. H. Press, S. A. Teukolsky, W. T. Vetterling, and B. P. Flannery, "Numerical Recipes", Cambridge Univ. Press, 2001.

[14] M.C. Jeruchim, P. Balaban, and K.S. Shanmugan, *Simulation of Commincation Systems*, Kluwer Academic/ Plenum Publishers, 2000.

[15] W.Weiershausen, H.Scholl, F. Kuppers, R. Leppla, B.Hein, H. Burkhard, E. Lach, and G. Veith, "*40Gbps field test on an installed fiber link with high PMD and investigation of differential group delay impact on the transmission performance*," in Proc. OFC'99, vol.3, San Diego, CA, 1999, Paper ThI5, pp125-127.

[16] P.A. Andrekson, "*40 Gbit/s soliton transmission on installed fiber lines*," in Proc. IEE Colloq. High Speed and Long Distance Transmission, Birmingham, UK, Mar. 1999.

[17] D. Marcuse, C.R. Menyuk, and P.K.A. Wai, "*Application of the Manakov-PMD*

Equation to Studies of Signal Propagation in Optical Fibers with Randomly Varying Birefringence," J. Lightwave Technol., vol. 15, pp. 1735-1746. Sept. 1997.

[18] G.P. Agrawal, *Application of Nonlinear Fiber Optics*. Academic Press, 2001.

[19] C.R. Menyuk, "*Application of multiple-length-scale methods to the study of optical fiber transmission*," J. of Eng. Math., vol 36, pp. 113-136, 1999.

[20] A. Galtarossa, L. Palmieri, M. Schiano and T. Tambosso, "*Statistical characterization of fiber random birefringence*", Opt. Lett., Vol.25, No.18, pp.1322-1324, Sept, 2000.

[21] P.K.A. Wai and C.R. menyuk, "*Polarization Mode Dispersion, Decorrelation, and Diffusion in Optical Fibers with Randomly Varying Birefringence*," J. Lightwave Technol., vol. 14, pp. 148-157, 1996.

[22] C. R. Giles and E. Desurvire, "*Propagation of signal and noise in concatenated erbium-doped fiber optical amplifier*", J. Lightwave Technol., vol. 9, Feb. 1991.